國立臺灣師範大學地球科學研究所

碩士論文

臺師大雙星散斑觀測計畫

Speckle Observation of Binary Stars at NTNU

指導教授：Hsieh-Hai Fu 傅學海

研究生：En-Wei Lin 林恩瑋

中華民國九十八年七月

Abstract

The binary image will be distorted by atmospheric turbulence, however the angular separation of a binary could be determined with speckle interferometry technology. The binary program with speckle interferometry at NTNU has been set up since 2002.

The commercial CCD, DMK 31AF03 CCD, is suitable for the binary program with the method of speckle interferometry. Because C-14 is the telescope with a moving primary mirror, it is not suitable for speckle observations.

There are 24 binaries chosen for our 2009 program, and the parameters of 13 binaries are determined. Their angular separations are between 0.61 ~ 8 arcsecs. The brightnesses of the primary stars fall between 1.93~5.64 mag.

摘　　要

　　大氣擾動會使得我們觀測到的雙星影像產生變形，然而透過散斑干涉技術，我們可以去測量出雙星系統的角距和方向角。從 2002 開始，臺師大建立雙星系統的散斑干涉觀測技術。

　　商業用的 CCD，DMK 31AF03 是我們這次雙星系統的散斑干涉觀測技術所使用的 CCD；由於 C-14 的主鏡會隨著望遠鏡移動時而變動，所以不適合作為雙星系統的散斑干涉觀測技術的工具。

　　在 2009 年的觀測計畫中，我們選定了 24 個雙星系統，而其中只有 13 個雙星系統被偵測出來，這些雙星的角距介在 0.61 到 8 角秒之間，主星的亮度介在 1.93 星等到 5.64 星等之間。

誌　　謝

Contents

List of Figures

List of Tables

1 Introduction

The binary image will be distorted by atmospheric turbulence so that the binary with angular separation less than seeing disk is hard to be determined. However, the binary with small angular separation could be determined with speckle interferometry technology. The method of speckle interferometry is typically used to close binary observation with angular separation smaller than 3 arcsecs and magnitude difference between primary and secondary is smaller than 3 or 4 mag. (such as Labeyrie, 1970, McAlister, 1976, Hartkopf, W. I., 1991, etc.).

Because of the turbulence of Earth's atmosphere, air density is varied with time quickly, so that the stellar light through the different spatial air cell produces many luminous spots, called speckle. The image of a point source on the focal plane of a telescope, such as a star, is distorted by the atmospheric smear or atmospheric turbulence, and it is unable to reach to the Airy disk. The angular resolution of optical observation is limited to seeing disk, rather than telescope, generally about $1''\sim 2''$ for good seeing, and $3''\sim 5''$ for bad seeing.

If the angular separation of a binary system larger than seeing disk, the primary and secondary will be recorded clearly, for example, Castor. In addition, the number of speckle could be counted in each frame (Fig. 1.1) with exposure time less than 0.033 seconds. There are about 14 speckles for the primary on the night of March 17, 2009, so that the air cell is about 10 cm for the aperture, 35 cm, of C-14. For the scale of $0.0689''$/pixel, the seeing is estimated about 2 arcsecs integrating 120 frames, ie., equivalent exposure time of 4 seconds (Fig. 1.2).
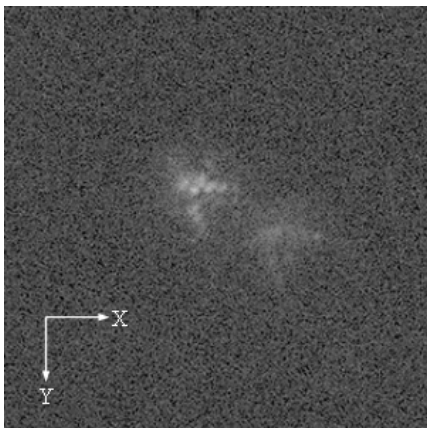
Fig. 1.1 Single frame with exposure time 1/60 sec of Castor with speckle ~ 0.4″
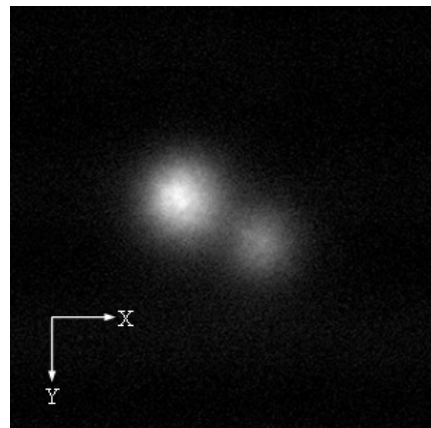
Fig. 1.2 The image exposure time 4.0 sec of Castor with seeing disk ~ 1.8″

If the angular separation between the primary and secondary less than seeing disk, such as HIP 43109, it is very difficult to find the two stars (Fig. 1.3). The image of pixel scale about 0.0689″/pixels with total size of image of about 20 arcsecs, and the seeing disk is about 2 arcsecs with the image in long exposure time of 4 seconds on the night of March 17, 2009 (Fig. 1.4).
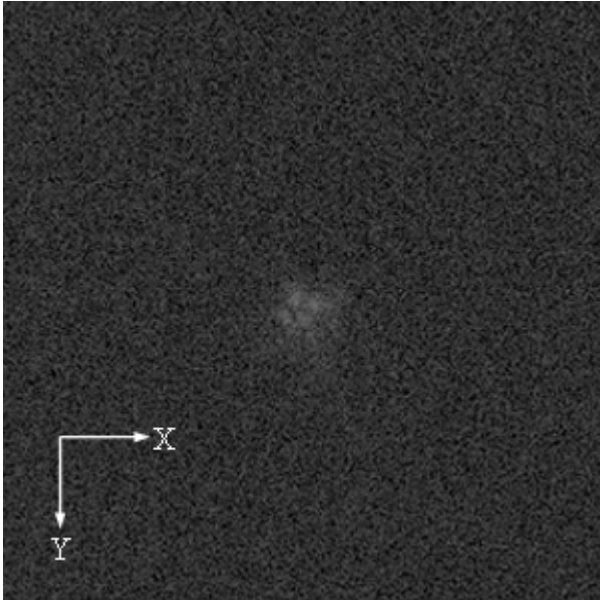
Fig. 1.3 Single frame with exposure time 1/60 sec of HIP 43109 with speckle ~ 0.6″
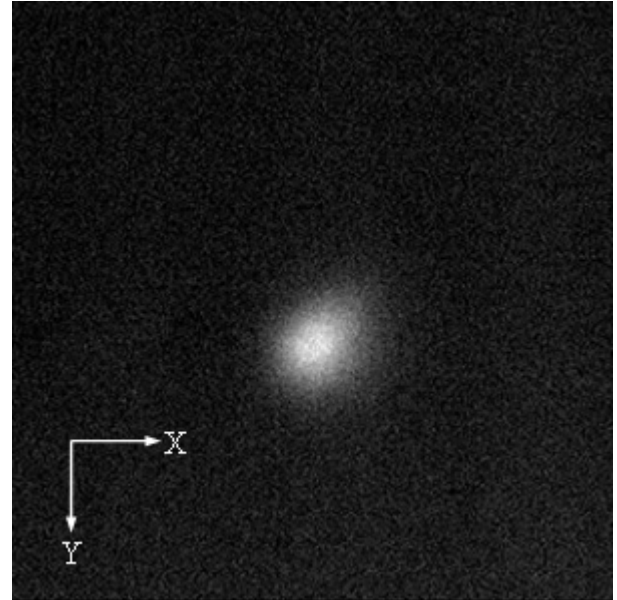
Fig. 1.4 The image exposure time 4.0 sec HIP 43109 with seeing disk 2.4″

Jean Texereau (1963) first described the speckle phenomena. He used eye-piece and sensitive photographic films with 193-cm telescope at Haute-Provence Paris. A point-like stellar image with very short exposure time, less than 0.03 seconds, is composed of numerous short-lived speckles, and the minimum size of a speckle is equivalent with the Airy disk, diffraction limit of a telescope.

Michelson & Pease (1921) was first in 1920-1921 used interferometry technology taking properties of light, and they succeeded to measure the angular diameter of a red supergiant star, Betelgeuse, using an astronomical interferometer on the Mount Wilson 100-inches telescope, and the base line up to 20-foot reaches an angular resolution to resolve about 0.02 arcsec.

In 1970, Labeyrie (1970) described a method can resolve atmospheric turbulence. The differential limitation of a telescope can be obtained by laser processing the speckle pattern with large telescope in short exposure. Labeyrie's technique of "speckle interferometry" uses high-magnification, short-exposure snapshots to freeze out the instantaneous effects of turbulence and then applies mathematical techniques to remove

the effect of turbulence (Labeyrie, 1970). The method of speckle interferometry superbly matched the needs for observations of binary star systems.

The speckle interferometric method is usually used for binary system with the angular separation less than 2″~3″ down to the resolution of the telescope (Gezari, Labeyrie, and Stachnik, 1972; Korff, Dryden, and Miller, 1972; Dainty, 1973; Liu and Lohmann, 1974; Knox and Thompson, 1974). After 1970s, it became an extremely active field scientifically with important contributions made to a wide range of topics in binary astrophysics (McAlister, 1981; Marchetti, Faraggiana, and Bonifacio, 2001; Baraffe, Chabrier, Allard, and Hauschildt, 1998).

There were many researchers developed the speckle interferometric method to measure the angular separation and the position for binary with freeze speckle pattern in term of 0.03 seconds or less exposure time. From 1977 until 1998, group of CHARA (The Center for High Angular Resolution Astronomy) of Georgia State University, USA carried out the most scientifically program in speckle interferometry which is applied to the study of binaries. Thousands measurements of binaries, including more than 300 systems that had never been previously resolved, had been published, and these measurements almost observed with instrumentation at 4-m class telescopes in Arizona and Chile (ex. McAlister et al., 1989; McAlister, 1993, Hartkopf et al., 1997, Bagnuolo et al., 2006).

Since around 2000, Many observatories with small telescopes less than 2-m developed the technology of speckle interfrometry to the observation of binary, such as U.S. Naval Observatory (USNO)(Muller et al.,2005, Muller et al.,2007), Calar Alto observatory, Spain (Boccaletti et al., 2001), Rutkowski and Waniak (2005), PISCO (Scardia et al., 2005, Scardia et al., 2007, Prieur et al., 2001), etc..

In USNO, the speckle interferometric method for binary observation with 0.66-m telescope was developed since 1990 (Germain et al., 1994; Mason et. al., 2006), and the CCD cameras are used as speckle image detectors, more sensitive and digitized data make speckle interfrometry imaging of binaries are much cheaper for small telescopes.

Furthermore, a 0.5-m telescope (Rutkowski, 2005), a 1.52-m telescope in Calar Alto observatory, Spain (Docobo et al., 2007) ,a 1-m telescope in Yunnan Observatory (Wang, Yi-Ming et al., 1988) ,and a 3.5 m telescope in the WIYN Observatory located at Kitt Peak, Arizona (Horch, Elliott et al., 1999) ,also did very precise observations of small separation binaries.

The webcam is also used for binary observation with speckle interferometric method (ex. Hsieh-Hai Fu and Yi-Cheng Yen, 2007; Schlimmer, 2007; Calloi, 2008; Horch et al., 2009).

In Taiwan, the first speckle interferometric observation of binaries was done in National Central University (Li, 1993). A 61-cm telescope was used to observe at least 4 targets (Antares, ADS 15971, ADS 1598, and Castor). The images were captured by an analog signal output CCD and were recorded with V8 tapes that were digitized by a frame grabber.

The binary program with the speckle interferometric method at campus of NTNU was developed since 2003 (Yan, 2007). Now, a CCD chip from the Image Source Company webcam is used to satisfy the requirement of speckle observations.

There are 22 binaries observed with C-14 and RCOS-16 telescopes at NTNU flat roof observatory. The objects shown in Table 2.1 are 10 binaries with the angular separation between 0.3″ and 5″, and Castor is chosen for checking the calibration of scale and angular separation.

The data of orbital elements of 11 binaries are taken from Sixth Catalog of Orbits of Visual Binary Stars (Hartkopf & Mason 2003)，and the orbit of each star is plotted in term of the orbital elements.

2 Observations

2-1 Equipment

A real time DMK 31AF03 CCD and two telescopes (Fig. 2.1), C-14 and RCOS-16 (Fig.2.2) in Flat Roof Observatory at campus of NTNU, are used in the binary program. A PJ 20 mm eyepiece is set in front of the focus plane to increase the focus length or enlarge the image.

C-14 is a type of Schmidt-Cassegrain telescope (the production of Celestron SCT's) with aperture of 14-inch (356mm), focal ratio of f/11, and it is rotated clockwise or counters clockwise to move the primary mirror forward or backward to adjust the focus. The telescope is mounted on a German Equatorial mount of Losmandy Titan Mount Head with the Gemini computer control system on the hand control box. The Gemini Control Panel inputs include provisions for communication by RS232/422 to a personal computer.

The RCOS-16 is type of Ritchey-Chretien Optical Systems with a Carbon Fiber Optical Tube, and the aperture is 16-inch (406mm), focal ratio of f/8.4. Its focus is matched by moving the secondary mirror in precise increments. RCOS-16 is mounted on a German Equatorial mount of Paramount 1100 ME. The software T-Point and The Sky 6 are used for increased pointing accuracy.

The DMK 31AF03 CCD (Fig. 2.3) of the Image Source Company, Germany, with IC Imaging Control software is used to record the speckle images of binary. The CCD chip is SONY ICX204al chip with 1024×768 square 4.65 μm pixels in 8-bit A/D converter. This type of CCD uses progressive scan that allows all pixels' signals to be output independently.

No filter was used for getting photons as much as possible. The wave length, 510 nm, is determined from the CCD characteristic curve, the maximum of the quantum effect (Fig. 2.4). In the period of observations, IC Imaging Control software is used to adjust some parameters for speckle observations such as brightness, gamma, gain, exposure time, and record format.

A mask of double slits (Fig. 2.5) made by Hsiao-Er Chuang (莊孝爾) is set in front of the telescope for determining the focal length.

Fig. 2.1 CCD installed with eyepiece (inside the tube) on C14

Fig. 2.2 CCD installed with eyepiece
(inside the tube) on RCOS 16

Fig. 2.3 DMK 31AF03 CCD
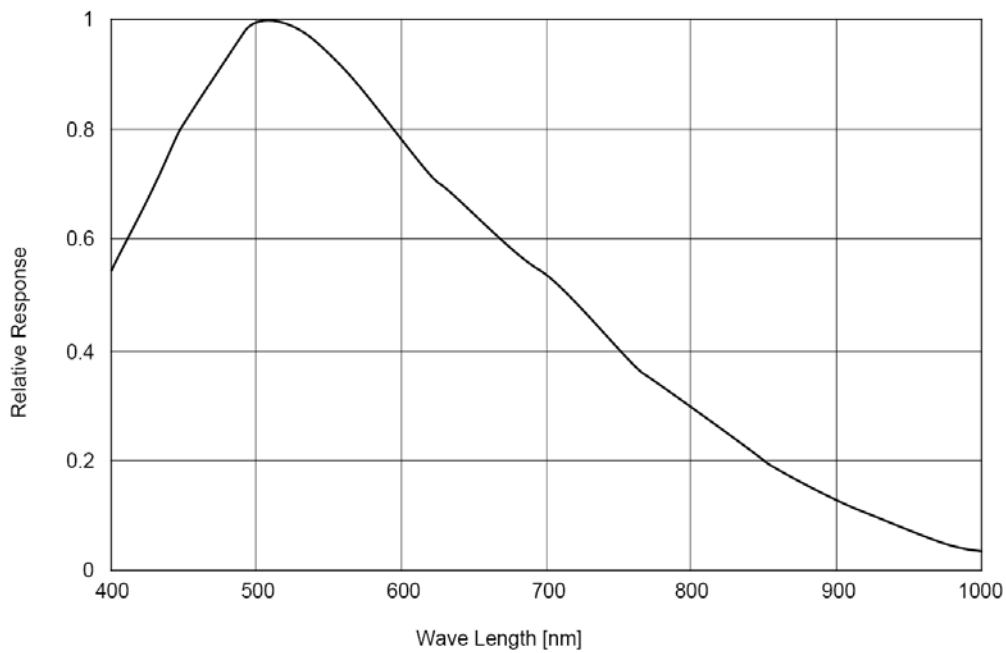
Fig. 2.4 CCD Spectral Sensitivity Characteristics
http://www.theimagingsource.com/downloads/icx204al.en_US.pdf

Fig. 2.5 The mask of double slits is set up on the telescope

2-2 Target list

The light pollution in Taipei city is serious and the short exposure time is restricted less than 0.33 seconds Thus the targets with the following characteristics are selected due to the instrumental and atmospheric limits:

• declination north of -20°,

• the primary or secondary is brighter than 6th magnitude in V

• magnitude difference between the primary and secondary smaller than 3 mag

• angular separation between 0.2 ~ 4"

The wide binary such as Castor was sometimes observed for integrating data and for checking the calibration of scale and orientation. 22 binary systems are chosen in total, and the basic data are taken from Sixth Catalog of Orbits of Visual Binary Stars (Hartkopf & Brian 2006) (Table 2.1). In Table 2.1, column 1 is the Name of discover designation and components, or other catalog designation, column 2 is ADS of Aitken Double Star catalog number, column 3 is HIP of Hipparcos catalog number, column 4 is RA of epoch-2000 (right ascension), column 5 is Dec of epoch-2000 (declination), column 6 is magnitude of the primary (usually in V band), and column 7 is magnitude of the secondary.

Table 2.1 Data of the selected binaries			RA			Dec			V1	V2
Name	ADS	HIP	(h	m	s)	(°	′	″)	V1	V2
MKT 1Aa	94	677	08	00	24	+ 29	05	27	2.22	4.21
STT 515AB	940	5434	01	09	30	+47	14	30	4.59	5.61
ANJ1Aa	3841	24608	05	16	41	+ 45	59	59	0.08	0.18
STF774Aa,B	4263	26727	05	40	45	- 01	56	33	1.88	3.7
Castor	6175	36850	07	34	36	+ 31	53	32	1.93	2.97
SP1AB	6993	43109	08	46	46	+ 06	25	08	3.8	5.3
STT208	7545	48402	09	52	06	+ 54	03	51	5.28	5.39
HU879	7780	51233	10	27	53	+ 36	42	27	4.62	6.04
STF1523AB	8119	55203	11	18	10	+ 31	31	45	4.33	4.8
STF1670AB	8630	61941	12	41	40	- 01	26	58	3.48	3.53
STF1728AB	8804	64241	13	09	59	+ 17	31	45	4.85	5.53
STF1865AB	9343	71795	14	41	09	+ 13	43	42	4.46	4.55
STF1937AB	9617	75312	15	23	12	+ 30	17	18	5.64	5.95
JEF1	HR5747	75695	15	27	50	+ 29	06	20	3.68	5.2
HU580AB	9744	76852	15	41	33	+ 19	40	14	5.35	5.22
STF1967	9757	76952	15	42	45	+ 26	17	44	4.04	5.6
CHR259	HR5881	77516	15	49	37	- 03	25	49	3.75	5.39
STF2140Aa-B	10418	84345	17	14	39	+ 14	23	25	3.48	5.4
STF2272AB	11046	88601	18	05	27	+ 02	30	09	4.22	6.2
MCA 55Aac	12540	95947	19	30	43	+ 27	57	35	3.37	5.16
BLA 6	HR7536	97365	19	47	23	+ 18	32	03	4.32	4.95
BU 151AB	14073	101769	20	37	32	+ 14	35	42	4.11	5.02
STF2727	14279	102531	20	46	38	+ 16	07	26	4.36	5.03
STF2909	15971	110960	22	28	49	- 00	01	12	4.34	4.49

From Sixth Catalog of Orbits of Visual Binary Stars (Hartkopf & Brian 2006),

http://ad.usno.navy.mil/proj/WDS/orb6/

2-3 Speckle observation mode

Speckle observations for binary at the NTNU FRO were carried out four nights, March 17, 2009, April 23, 2009, May 29, 2009, June 29, 2009, and July 23, 2009. A series of speckle images of the binary are recorded to a personal computer or notebook in avi format with 15 or 30 frames per second. The image bandwidth with full frame is 1024 pixels × 768 pixels. The record time in each frame is less than 1/30, 1/45 or 1/60

second. A PJ 20-mm eyepiece was used to decrease pixel scale. Usually, two thousand frames are required for recording speckle images of a single target. The value of gain will be adjusted, depending on the rate of signal/noise of image of each binary.

In order to determine the scale of a pixel, a mask of double slits is set in front of the telescope to produce interference pattern on focal plane, and the intervals of a set of fringes depends on the separation of two slits. The scale, α is defined using the formula:

$$\alpha \ (''/\text{pixel}) = 206265 \frac{\lambda}{d \ \Delta y} \ ,$$

where α is the separation scale in arcseconds per pixel, λ is the effective wavelength, d is the separation of two slits and is the mean spacing in pixels between peaks of fringes.

In order to determine the orientation of the image frame to find position angle, a set of images of a bright star is recorded with stopping telescope's tracking system. The star tracking from east to west in a straight line is used for determining the orientation of north.

After the date of June 1, 2009, RCOS-16 is used for observation of the binary program. There are two advantages for using RCOS-16. First, it is larger than C-14 with more light gathering power. Second, the focus system of ROCS-16 is much better than that of C-14, saving a lot of time, and increasing the accuracy of scale.

3 Data reduction

The video of speckle images of each star recorded in AVI format will be divided in to a series of single frame, xi, in bmp format, where i is the number of the ith frame. The data reduction for each star is processed in the following three steps:

1. The 2D-FFT in IDL (Interactive Data Language from Research Systems, Inc) language is used to transfer each frame, x_i, of speckle image to fx_i (Fig.3.2).

2. Sum of all fx_i images to a single image, $sum(fx_i)$ (Fig.3.3).

3. The 2D-FFT transfer image, $sum(fx_i)$, to final image, $ff(x)$ (Fig.3.4).

If the result image appears the obvious fringes, the $ff(x)$ image is used for determining relative coordinates of the secondary via the primary, and the angular separation and position angle of a binary system will be found from the coordinates after calibration.

3-1 Image process

Before analysis, the AVI format speckle film of a binary must be separated to a series of images in BMP format, and then these images are processed using IDL to find the coordinates of secondary relative to primary.

The specifications of the personal computer are: Intel(R) Core 2 Duo E6550 CPU 2.3 GHz, Gigabyte GA-P35-DS3 Motherboard, and 3.5GB RAM DDR2-800 DDR2 SDRAM. The computer's OS is Microsoft Windows XP Professional Service Pack 3.

The speckle images stream in AVI format are separated to a series of images in BMP format using a freeware of VirtualDubMod download from website of Avery Lee's VirtualDub,

VirtualDubMod is the improved version of VirtualDub. Besides VirtualDub original editing movie function, it can also expand avi format to single frames. It is licensed under the GPL. VirtualDubMod is hosted on SourceForge and the current version 1.5.10.2 is released on 29 August 2005. The single frame (Fig. 3.1) is separated from AVI to BMP files.

IDL is a popular data analysis language among scientists, and it is commonly used for interactive processing of large amounts of data including image processing.

3-2 The process of FFT and relative angular separation and position angle

2D-FFT is used to do the work of the speckle images of binaries, and to determine the parameters of angular separation (ρ) and position angle (θ). The intensity of image is discrete value rather than continuing curve, so that actually the Discrete Fast Fourier Transform is used in this work. The word 2D-FFT used previously means Discrete 2D-FFT.

Discrete Fourier Transform:

$$F(u,v) = \frac{1}{MN} \sum_{x=0}^{M-1} \sum_{y=0}^{N-1} f(x,y) e^{i2\pi(\frac{ux}{M}+\frac{vy}{N})} \qquad \text{…........ 3.1}$$

The information of binary system will be determined in terms of speckle image processed with IDL.

1. The quality of some frames separated from AVI movie clip is too bad, too faint or even having not speckle pattern, to use. Usually, there are about 200 frames of good quality with obvious speckle pattern that are chosen from the 2000 original frames to the final data reduction.

2. In order to save time, the original images of 1024 pixels×768 pixels are cut to the suitable square image of 300 pixels×300 pixels or 600 pixels×600 pixels, delete the un-necessary background.

3. Each bmp frames of speckle pattern is proceeding with the 2D-Fast Fourier Transform (2D-FFT) (Fig. 3.2) of IDL, and then sum all 2D-FFT images (Fig. 3.3) to find the fringes.

4. If the image of fringes is good, the process of 2D-FFT will do again to convert the interferometric pattern to the binary image with a mirror image (Fig 3.4), and the relative position of secondary relative to the primary are determined.
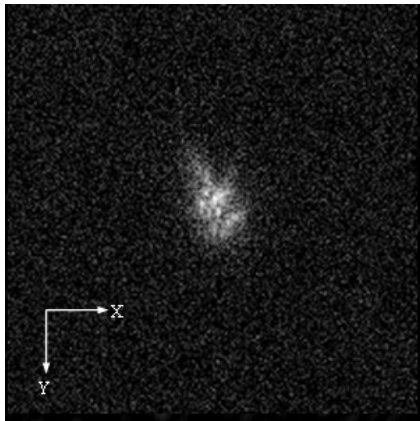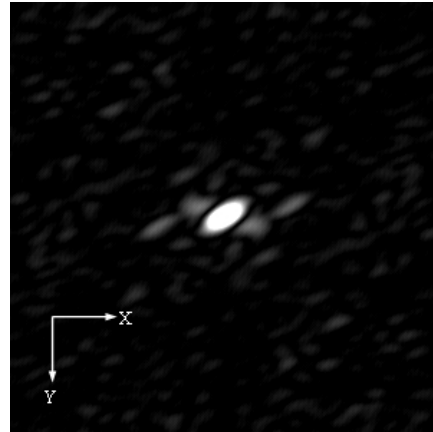
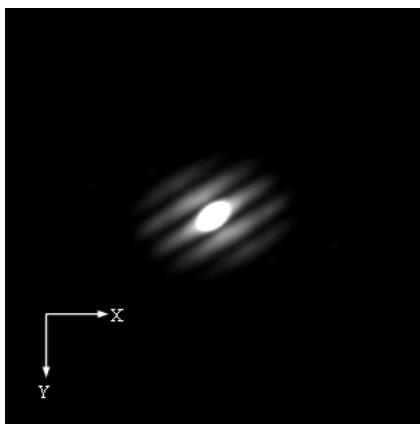Fig. 3.1 An original single frame,x_i

Fig. 3.2 FFT of Fig. 3.1, fx_i

Fig.3.3 Sum of Fig. 3.2, $sum(fx_i)$
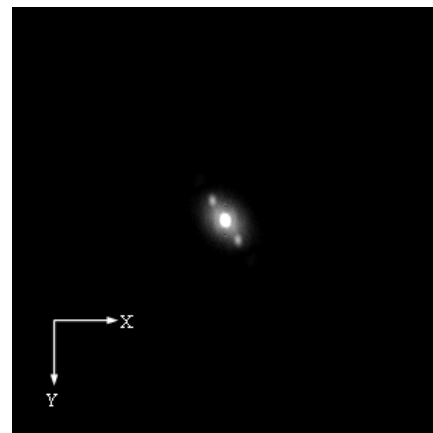

Fig.3.4 FFT of Fig. 3.3, ff(x)

5. After the process of 2D-FFT, the coordinates in pixels of the secondary relative to primary (150,150) is determined from the contour map of the images. The ρ in pixels is the distance between primary and secondary, and θ is measured from the y-axis (Fig 3.5).
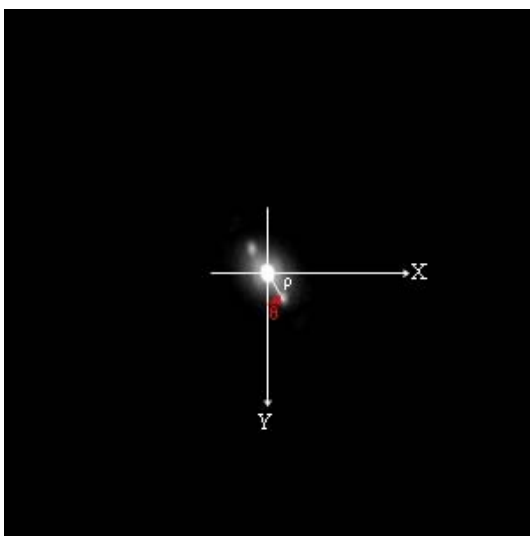

Fig.3.5 the relation of ρ and θ with the process of 2D-FFT.

4 Calibration

There are two methods of calibration used for this work. One is using the tracking image for orientation calibration and a mask of double slit for scale calibration. The other is using a wide binary, Castor, for both calibration of scale and orientation.

4-1 Scale and Young's double slits

In order to find the pixel scale correctly, a mask of double slits is set in front of the telescope and images of a bright star on focal plane are recorded.

The mask of double slits is set in front of C-14 and RCOS-16, respectively. The diffractive images of Young's double slits are processed as same as the process in Section 3-2, and the interval of the peak intensity in the interference pattern is found. In Young's double slit formula (Eq. 4.1),

$$d \sin \theta = n \lambda \quad \text{……………………..…………4.1,}$$

where d (mm) is the separation of double slits, λ (mm) is effective wavelength of CCD with most sensitive quantum effect, and n is the number of bright stripe of interference pattern from the central stripe, and let n = 1, here. According to the Spectral Sensitivity Characteristics of the CCD chip from the manual, the maximum quantum efficiency wavelength is about 510 nm (Fig. 2.4) and effective wavelength is set to 510 nm = 0.00051 mm.

If the focal length, f (mm) is much longer than d, i.e., θ is much small, then sin θ = tan θ and

$$\tan \theta = \frac{\Delta y}{f} \quad \text{………………………4.2,}$$

where Δy is interval of interference pattern in pixel measured from the fringes of a bright star, and it will be convert to unit in mm using the scale of CCD chip, 4.65 μm = 0.00465 mm per pixel. Substituting the eq. 4.2 into eq. 4.1, the formula will be:

$$d = \frac{f \cdot \lambda}{\Delta y} \quad \text{in mm ………………4.3,}$$

Let α be the scale in arcseconds per pixel, see Fig .4.1. Because the size of 1 pixel is much less than f, i.e., α is very small, so that

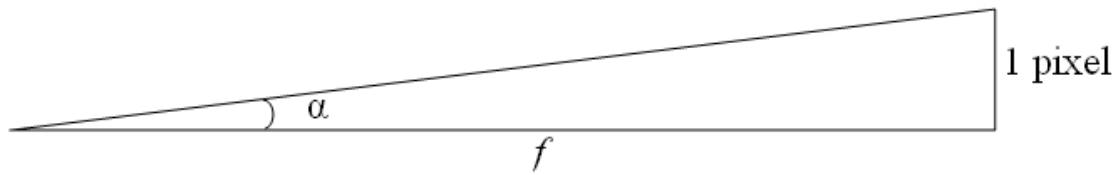Fig. 4.1 the angle, α (″/pixel)

$$\tan \alpha \approx \alpha = \frac{1}{f} = \frac{\lambda(mm)}{d(mm) \cdot \Delta y(pixel)} \quad (radian/pixel) \quad ....\text{........}4.4$$

$$\alpha = \frac{180 \times 60 \times 60}{\pi} \frac{\lambda(mm)}{d(mm) \cdot \Delta y(pixel)} = 206265 \frac{\lambda}{d \ \Delta y} \ (″/pixel) \ .....4.5$$

The primary mirror of C-14 will be shifted a little when the telescope point to other star and the focal length is then changed, so that the scale of C-14 calculated from the fringes of double slits is useless.

For RCOS-16, the separation scale, α in arcseconds per pixel, is determined from the method of Young's double slits. The separation of the double slits on the mask is set to 16.5 cm, 18.5 cm, 20.5 cm, 22.5 cm, and 24.5 cm in front of RCOS-16, (for example, the fringes of d = 25 cm shown in Fig. 4.2) and the values of Δy are 25.25 pixels, 23.20 pixels, 20.62 pixels, 19.33 pixels, and 17.94 pixels.

d (mm)	165	185	205	225	245
Δy (pixel)	22.25	23.20	20.62	19.33	17.94

The scale, α = 0.0271 ± 0.00053 ″/pixel for λ = 0.000510 mm for the images taken on the night of June 29, 2009.
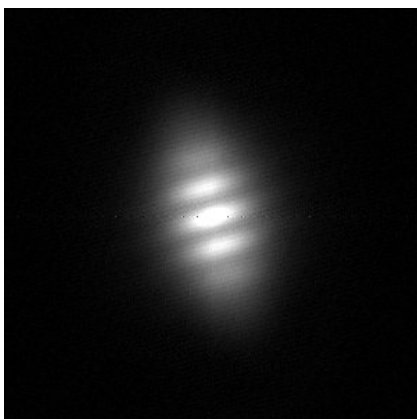

Fig. 4.2 The separation of the double slits set in front of RCOS-16. For example, the left image is 20.5 cm of the interval of the double slits.

4-2 The direction of north determined from stellar tracking

The position angle is the angle between the north and the line between the secondary with respect to the primary, and it is measured in degrees from north via east. For the binary observation, the orientation is determined using the image of a bright star taken by turning off the telescope tracking switch, and let the star drift through the whole field. The image of tracking overlapped about 100 frames is shown in Fig. 4.6. Capella and Arcturus are used in this observational season.

The direction of east-west is determined by linear regress of the tracking image. The same image process is used for tracking image, transferring AVI format to a series images in BMP format with VirtualDubMod free software. All about 100 frames of tracking image are processed by sum of them in average mode. The pixels with intensity value of maximum, 255, are selected, and then the coordinate of these selected pixels, ζ and η, are used for fitting straight line. The equation, $\eta = p\,\zeta + q$, fitted with linear regress is as the direction of east-west, where p and q are fitting constants.

The equation of stop tracking with C-14 is $\eta = (-0.0451 \pm 0.00100)\,\zeta + (154.0162 \pm 0.42966)$, then the angle relative to the ζ-axis of CCD chip is $2.58° \pm 0.06°$ (Fig. 4.3)
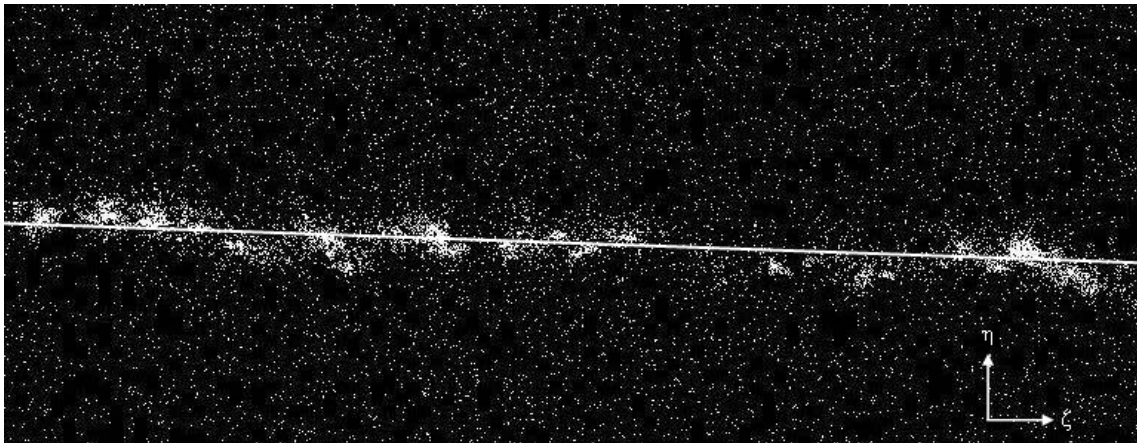

Fig. 4.3 The image of stop tracking with C-14 on the night of March 17, 2009

The equation of stop tracking with RCOS-16 is $\eta = (0.0652 \pm 0.00188)\,\zeta + (136.5856 \pm 0.98718)$, then the angle relative to the ζ-axis of CCD chip is $3.73° \pm 0.107°$ (Fig. 4.4)
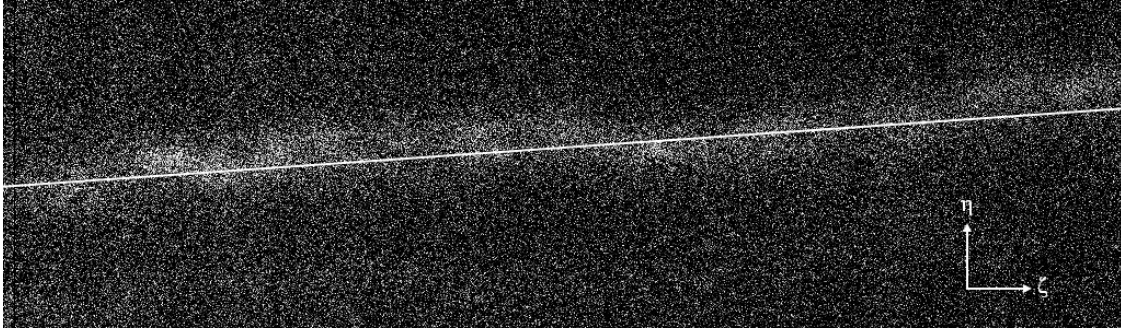
Fig. 4.4 The image of stop tracking with RCOS-16 on the night of June 29, 2009

4-3 Calibrations in term of a wide binary, Castor

For telescope C-14, the image of Young's double slits is not suitable for the calibration of scale, because the focal length of C-14 will be changed after the telescope moves to the other star. A wild binary system with good observations and data is used for scale calibration.

Castor (α Gem, WDS07346+3153=ADS 6175) is used for scale calibration of angular separation and the orientation, because this binary system has many good observational data in the Fourth Interferometric Catalog (Harkhopf and McAlister, 1998). The liner regress method is used to the angular-separation time and position-angle -time, respectively (Fig. 4.5 and Fig. 4.6), and the equations are listed in eq.4.7 and eq.4.8.

Calculated from equation 4.7 and equation 4.8, the angular separation and the position angle of Castor (Fig. 4.5 and Fig. 4.6) are

$\rho = 4.53''\pm 0.0419''$ and $\theta = 59.31°\pm 0.5119°$ at 2009.2081,

$\rho = 4.54'' \pm 0.0419''$ and $\theta = 59.28° \pm 0.5119°$.at 2009.3094.

The values of angular separation and the position angle of Castor at 2009.2081 and 2009.3094 are listed in Table 4.1. At 2009.2081, The angular separation between Castor A and B is 64.55 pixels and the angle relative to the x-axis of CCD chip is 58.2°, so that the angular scale is 0.0689 ″/pixel and the difference between the direction of north and the y-axis is 1.1° (Fig. 4.7). At 2009.3094, the angular separation between Castor A and B is 85.02 pixels and the angle relative to the x-axis is 49.7°, so that the angular scale is 0.0524 ″/pixel and the direction of north and the y-axis is 9.6° (Fig. 4.8).
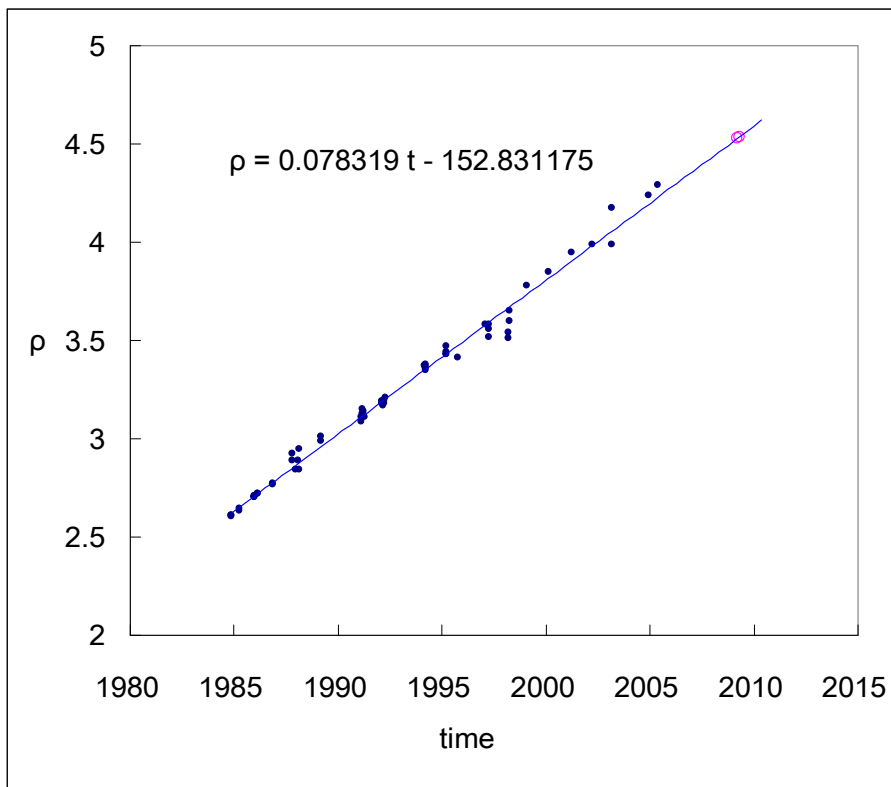
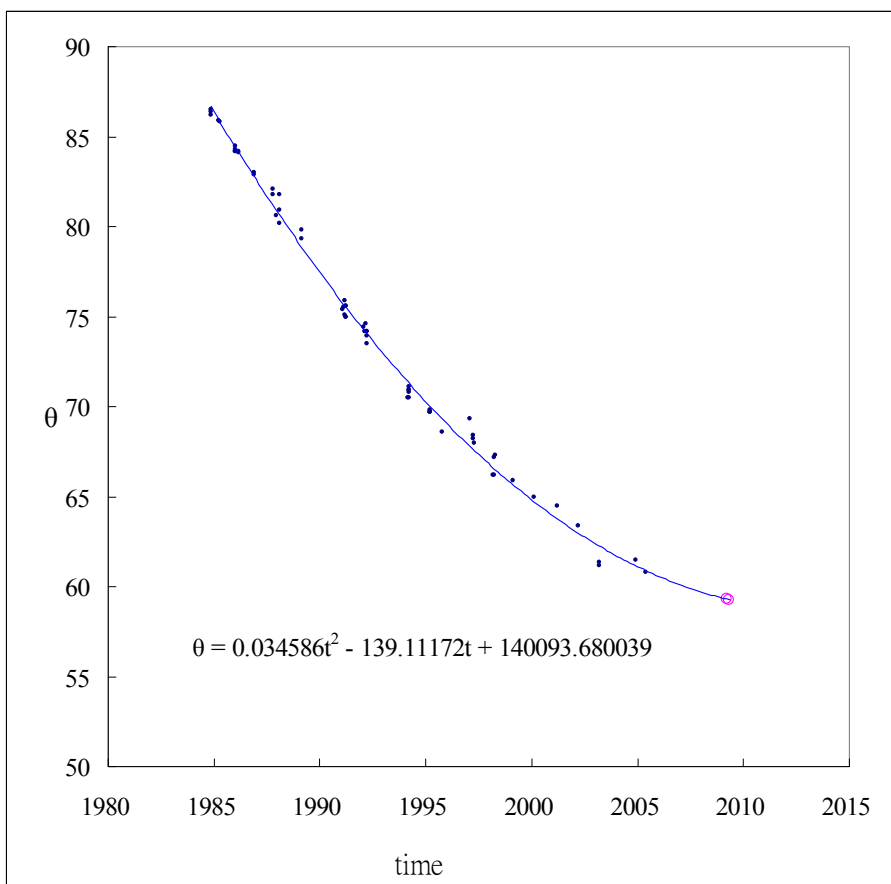Fig. 4.5 The angular separation of Castor at 2009.2081 and 2009.3094

Fig. 4.6 The position angle of Castor at 2009.2081 and 2009.3094

17

$$\rho = 0.078319\, t - 152.831175 \qquad\qquad \text{………4.7}$$

$$\theta = 0.034586\, t^2 - 139.111721\, t + 140093.680039 \qquad \text{………4.8}$$

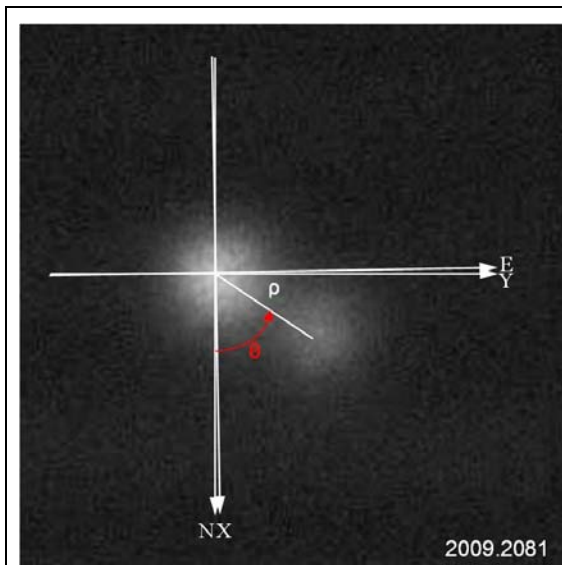| Table 4.1 Calibration with Castor						
time	Calculation		observation		Scale ("/pixel)	Orientation corrected
	$\rho(\prime\prime)$ eq. 4.7	$\theta(°)$ via NP eq. 4.8	ρ(pixel) with Castor	$\theta(°)$ via x-axis star tracking		
2009.2081	4.53 ±0.0419	59.3 ±0.52	64.5564	58.2	0.0689	-1.1°
2009.3094	4.54 ±0.0419	59.3 ±0.51	85.0145	47.9	0.0524	+11.35°

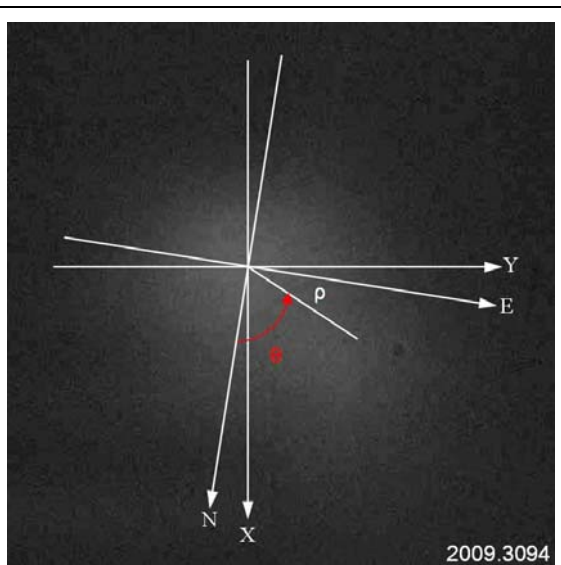| Fig. 4.7 The angle responds to y-axis and the angular scale at 2009.2081 the difference between the direction of north and y-axis.	Fig. 4.8 The angle responds to y-axis and the angular scale at 2009.3094 the difference between the direction of north and y-axis.

On March 17, 2009, the interferometric pattern of double slits and stellar tracking were used for calibrated ρ and θ. The calibration scale from interferometric pattern of double slits was different from Castor. The error is about 10% or more, too large to use. The value of ρ taken from Castor as scale, and the value of θ calculated from stellar tracking is used for calibration of orientation.

Table 4.2 Calibration with Castor and stellar tracking				
time	ρ(″) of calculation from eq. 4.7	ρ(pixel) of observation with Castor	Scale (″/pixel)	Orientation of via x-axis
2009.2081	4.53 ± 0.0419	64.5564	0.0689	+2.58°

On April 23, 2009, there were no observation with a double slits mask and stellar tracking, so that both calibration of scale and orientation calibrated from the data of Castor in the Fourth Interferometric Catalog.

Table 4.3 Calibration with Castor						
time	Calculation		observation		Scale (″/pixel)	Orientation corrected
	ρ(″) eq. 4.7	θ(°) via NP eq. 4.8	ρ(pixel) with Castor	θ(°) via x-axis star tracking		
2009.3094	4.54 ±0.0419	59.3 ±0.51	85.0145	47.9	0.0524	+11.35°

On June 29, 2009, the interferometric pattern of double slits and stellar tracking were used for calibration of scale and orientation.

Table 4.4 Calibration with double slits and stellar tracking		
time	Scale calculated from the fringes of double slits	Orientation of via y-axis
2009.4079	0.0271(″/pixel)	3.67°

5 Results

5-1 ρ and θ of the binary

The observations at the NTNU FRO were taken on March 17, 2009 and April 23, 2009. There are 12 binary systems detected after the FFT (Fig. 5.1) is calculated.The results of angular separation (ρ) and position angle (θ) are listed in Table 5.1 and Table 5.2. The results before 2009 June come from the observations made with C-14.

On June 29, 2009, the observations used RCOS-16, there are 2 binary systems detected after FFT (Fig. 5.2) calculations, the ρ and θare listed in Table 5.3. The scale of focal length was taken from the result of the double slits set in front of RCOS-16, and the orientation was determined from the image of stellar tracking.
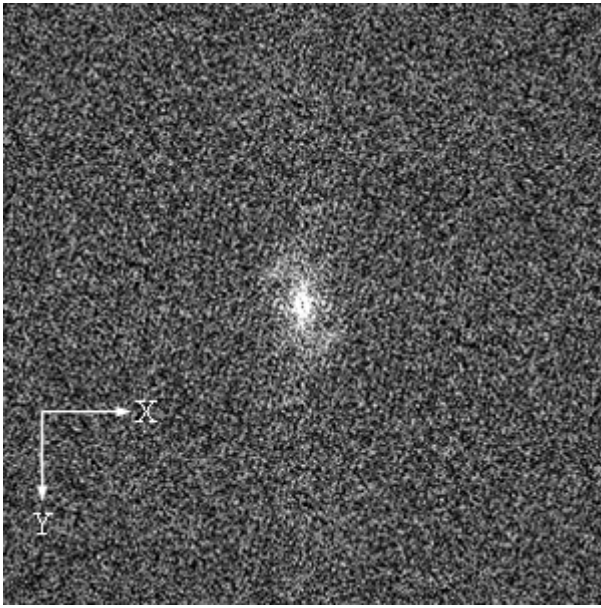
The orbit of each binary with observed data in this work and data taken from the Fourth Interferometry Catalog are plotted in Fig. 5.3.

Fig. 5.1 The result of observation with C-14
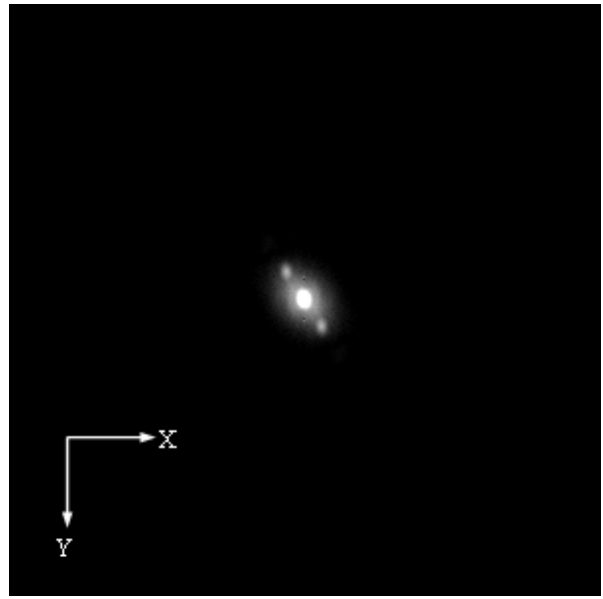The result of observation in March 17, 2009
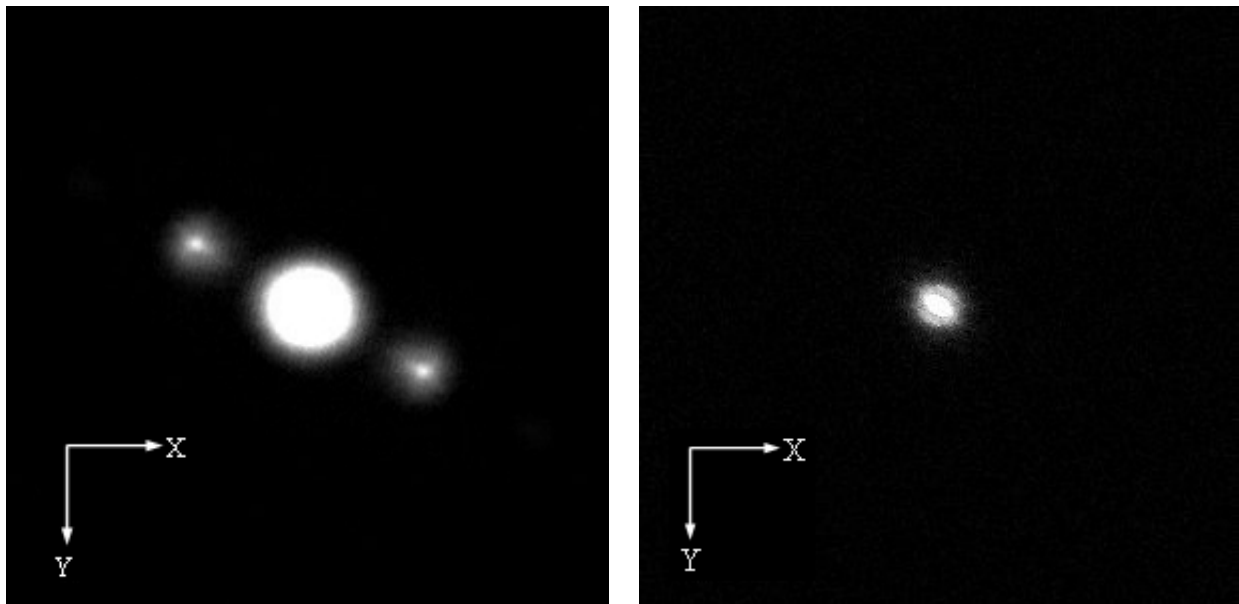
Castor   HIP 43109
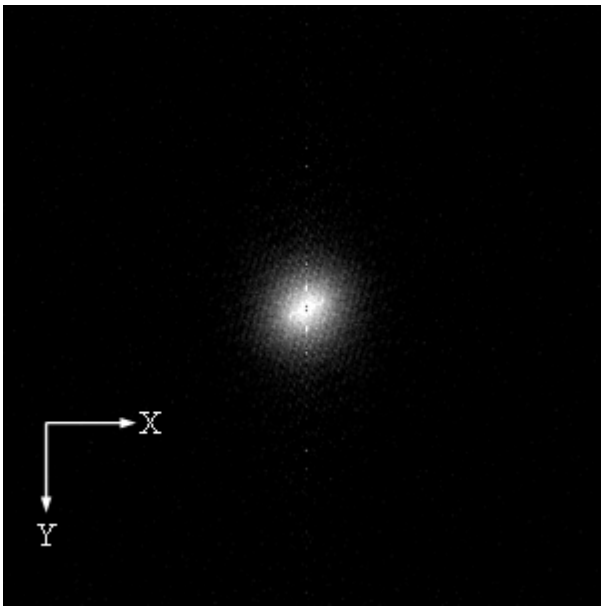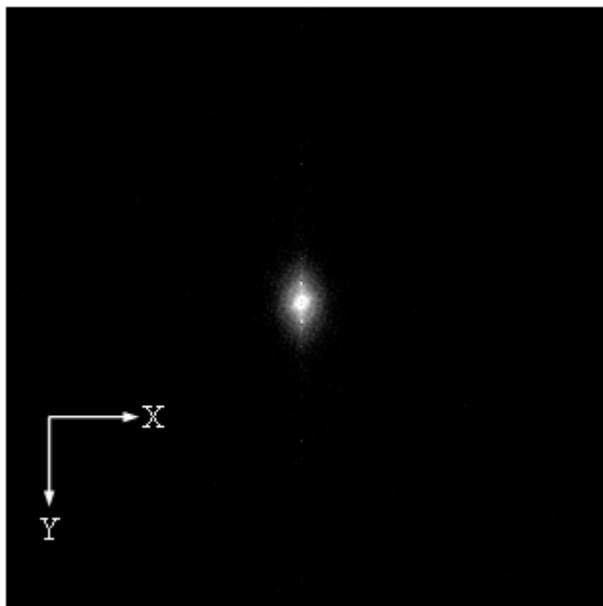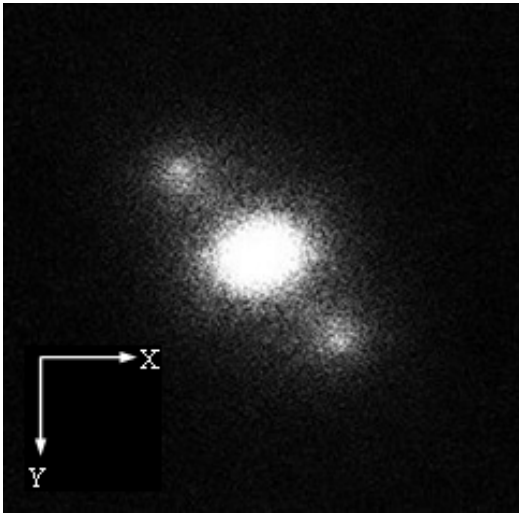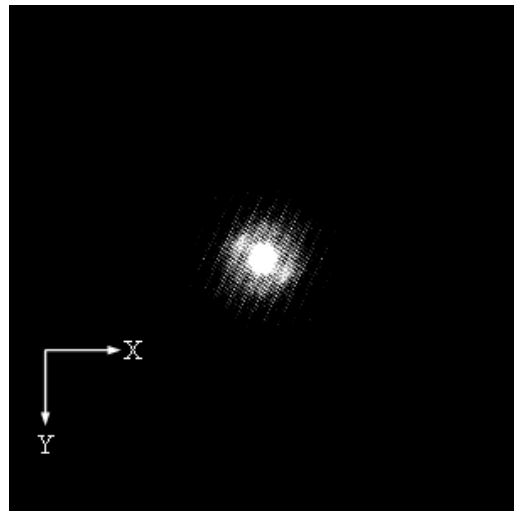
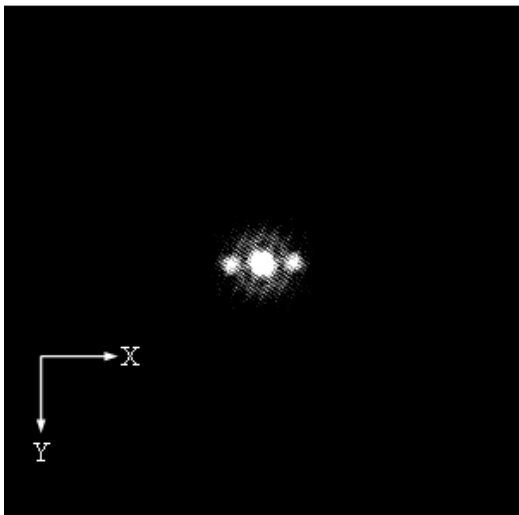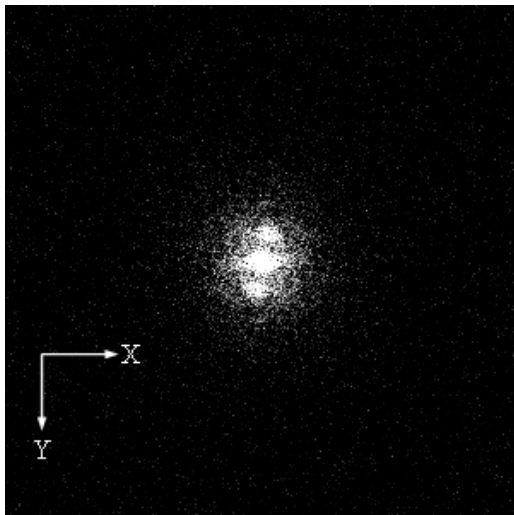HIP 55203

HIP 61941

HIP 71795
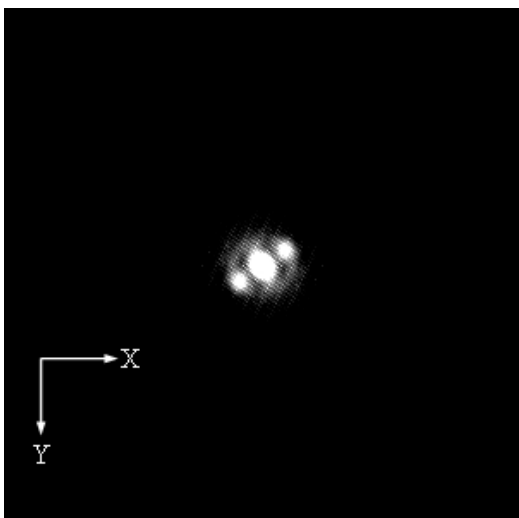

HIP 75695

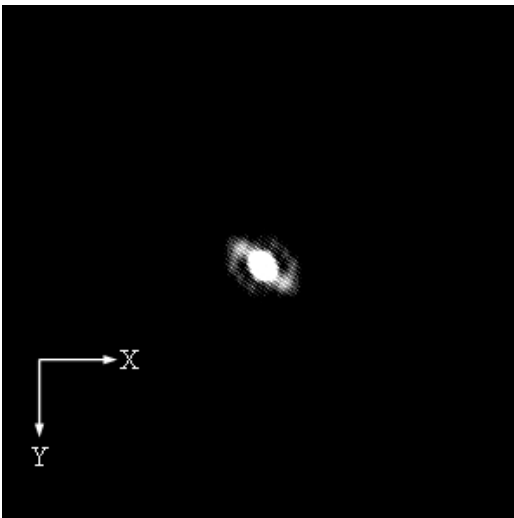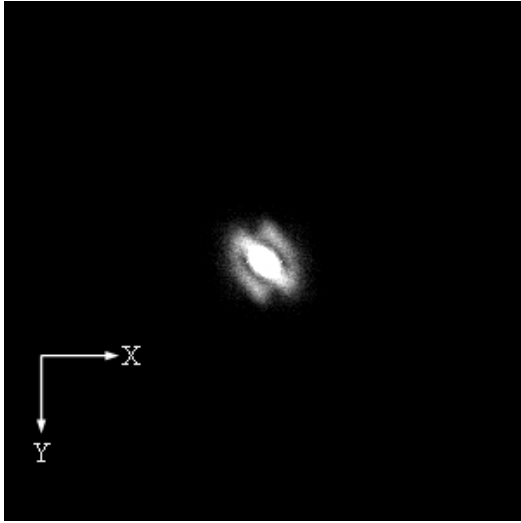The result of observation in April 23, 2009

Castor

HIP 51233

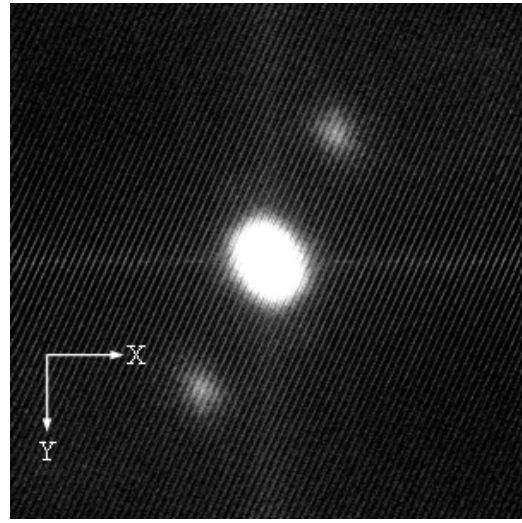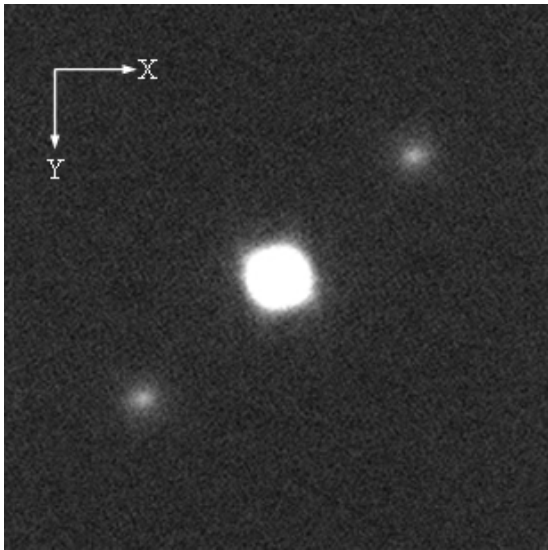HIP 64241

HIP 71795

HIP 75312

HIP 76852

HIP 76952

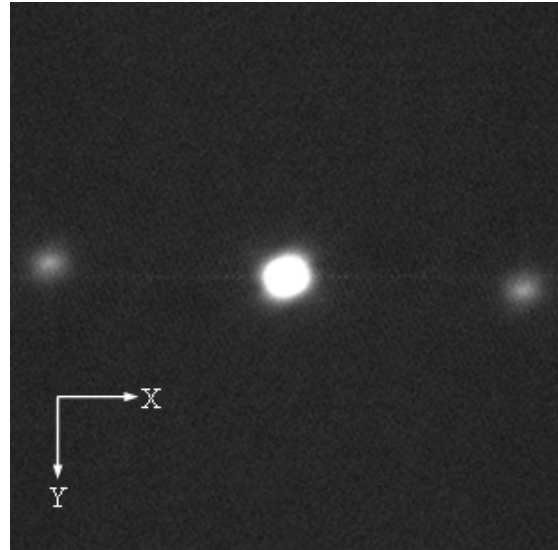HIP 88601

Fig. 5.2 The result of observation with RCOS-16
The result of observation in June 29, 2009

HIP 88601

HIP 102531

WDS	Name	ADS	HIP	″	°	notes
Table 5.1 The result of observation with C-14 in March 17, 2009						
05167+4600	ANJ 1Aa	3841	24608			fail
05407-0157	STF 774Aa,B	4263	26727			fail
07346+3153	Castor	6175	36850	4.53	63.12	*
08468+0625	SP 1AB	6993	43109	0.48	143.02	
10279+3642	HU 879	7780	51233			fail
11182+3132	STF1523AB	8119	55203	1.30	216.13	
12417-0127	STF1670AB	8630	61941	1.12	35.61	
13100+1732	STF1728AB	8804	64241			fail
14411+1344	STF1865AB	9343	71795	0.56	292.87	
15278+2906	JEF 1	HR5747	75695	0.41	146.31	fail
15427+2618	STF1967	9757	76952			fail
15496-0326	CHR 259	HR5881	77516			fail
17146+1423	STF2140Aa-B	10418	84345			fail
18055+0230	STF2272AB	11046	88601			fail
19307+2758	MCA 55Aac	12540	95947			fail

Used for calibration of the angular and the position angle.

WDS	Name	ADS	HIP	″	°	notes
Table 5.2 The result of observation with C-14 in April 23, 2009						
07346+3153	Castor	6175	36850	4.54	59.28	*
08468+0625	SP 1AB	6993	43109			fail
09521+5404	STT 208	7545	48402			fail
10279+3642	HU 879	7780	51233	0.69	226.96	
13100+1732	STF1728AB	8804	64241	0.8	102.39	
14411+1344	STF1865AB	9343	71795	0.76	293.73	
15232+3017	STF1937AB	9617	75312	0.8	136.85	
15416+1940	HU 580AB	9744	76852	0.8	248.01	
15427+2618	STF1967	9757	76952	0.61	134.87	
15496-0326	CHR 259	HR5881	77516			fail
18055+0230	STF2272AB	11046	88601	4.7	138.97	

Used for calibration of the angular and the position angle.

Table 5.3 The result of observation with RCOS-16 in June 29, 2009							
WDS	Name	ADS	HIP	″	°		notes
18055+0230	STF2272AB	11046	88601	5.3	135.5		
19474+1832	19474+1832	HR7536	97365				fail
20375+1436	20375+1436	14073	101769				fail
20467+1607	20467+1607	14279	102531	8.58	264.7		
22288-0001	22288-0001	15971	110960				fail

5-2 (O-C) in binary orbits

From Table 4.1, the scale and orientation obtained from Castor are used to find ρ and θ of other binary system on March 17, 2009, April, and May 29, 2009. On June 29, 2009, the ρ and θin Table 4.4 were obtained the RCOS-16 observations. The scale of focal length was taken from the result of the double slits set in front of RCOS-16, and the orientation was determined from the image of stellar tracking.

The binary orbit is plotted in terms of orbital elements taken from Sixth Catalog of Orbits of Visual Binary Stars (Hartkopf & Mason 2003), and the observed data are taken from the WDS 2006.5 version the Fourth Catalog of Interferometric Measurements of Binary Stars. In each plot of Fig 5.3, the open circle are the results of this work, black spots are the data in Fourth interferometric catalog, and "+" is the position of primary. (O-C) is the line between the mark (O) and the position at orbit (C).

Fig 5.3 The binary orbit of observation

HIP 43109   P=15.0507 years

HIP 55203   P=59.878 years

HIP 61941   P=169.18 years

HIP 71795   P=123.44 years
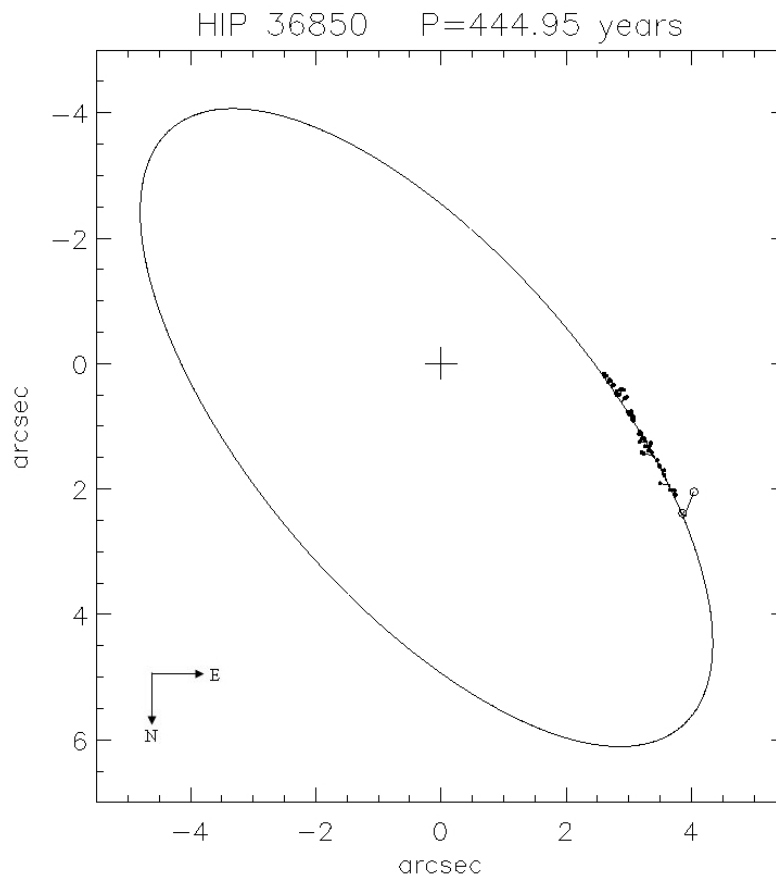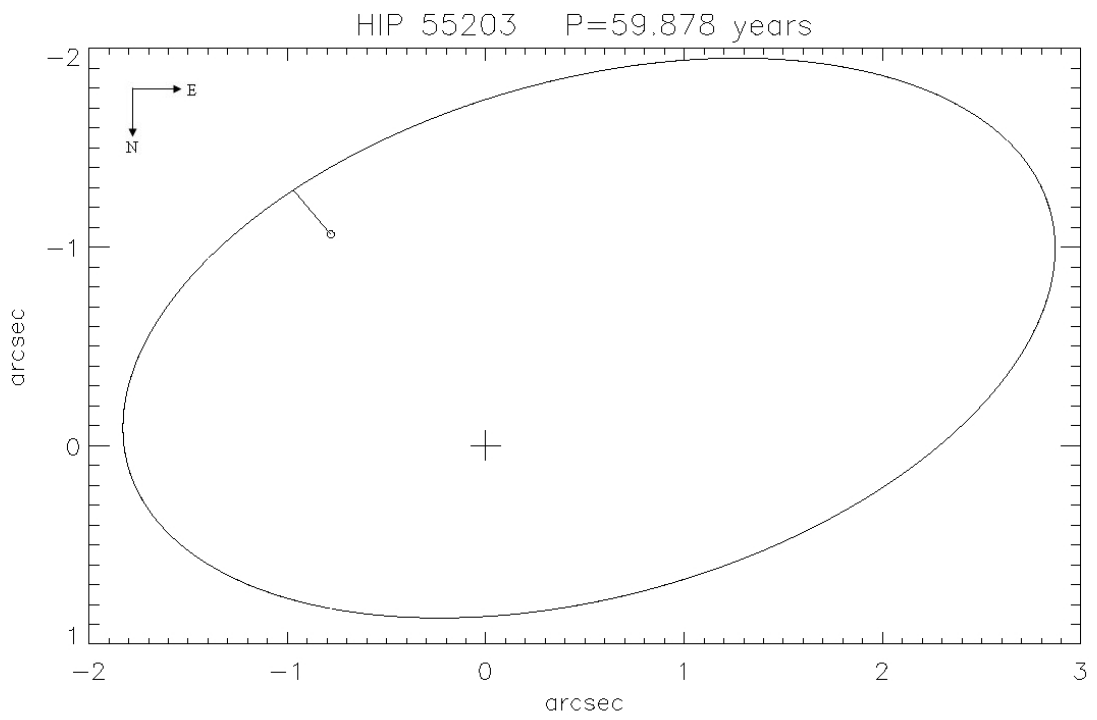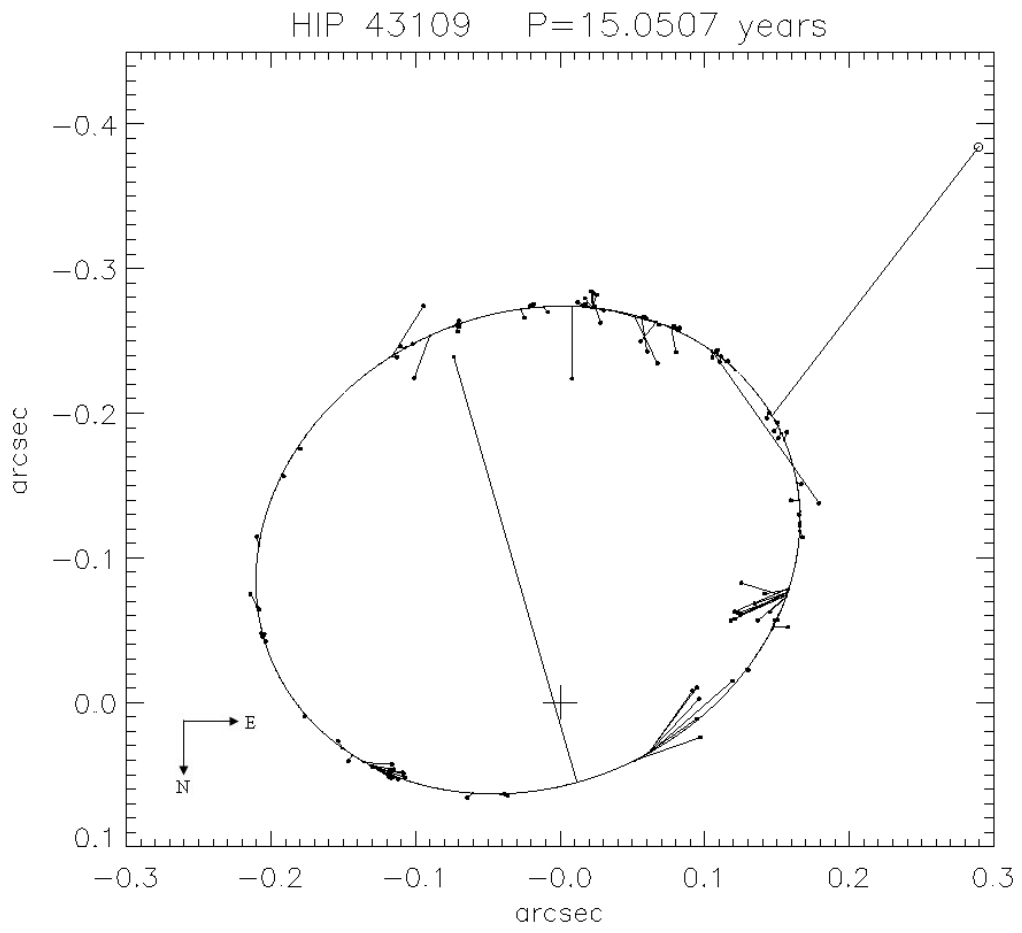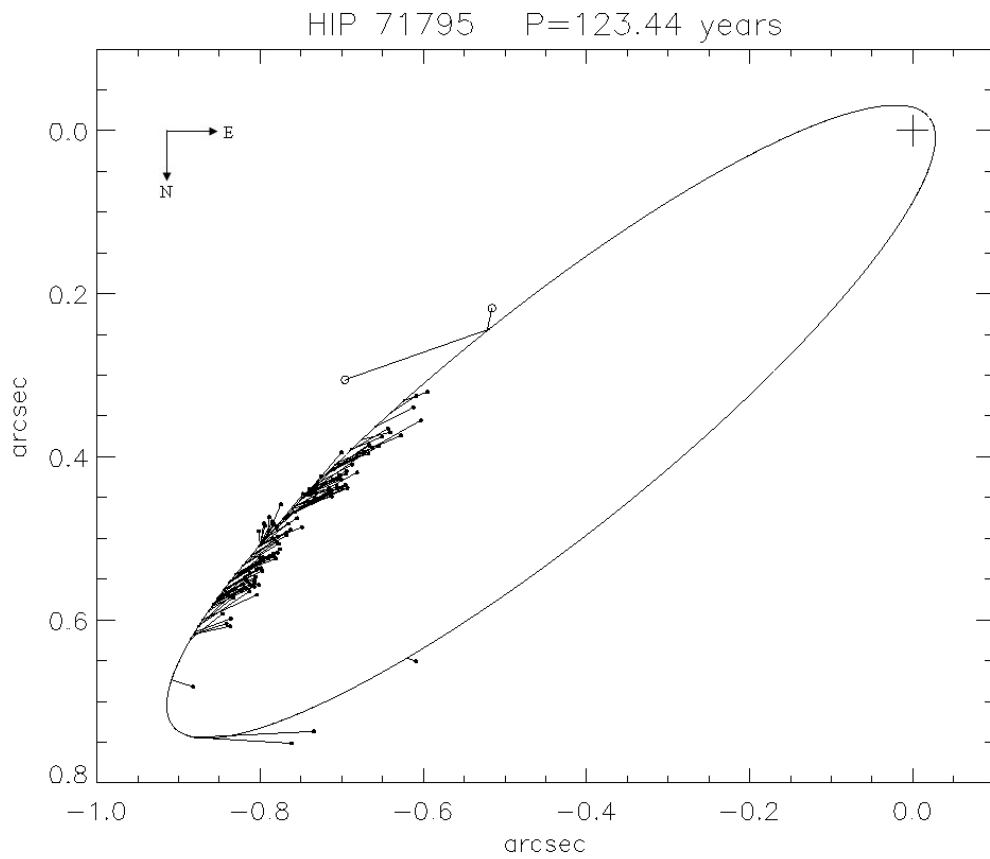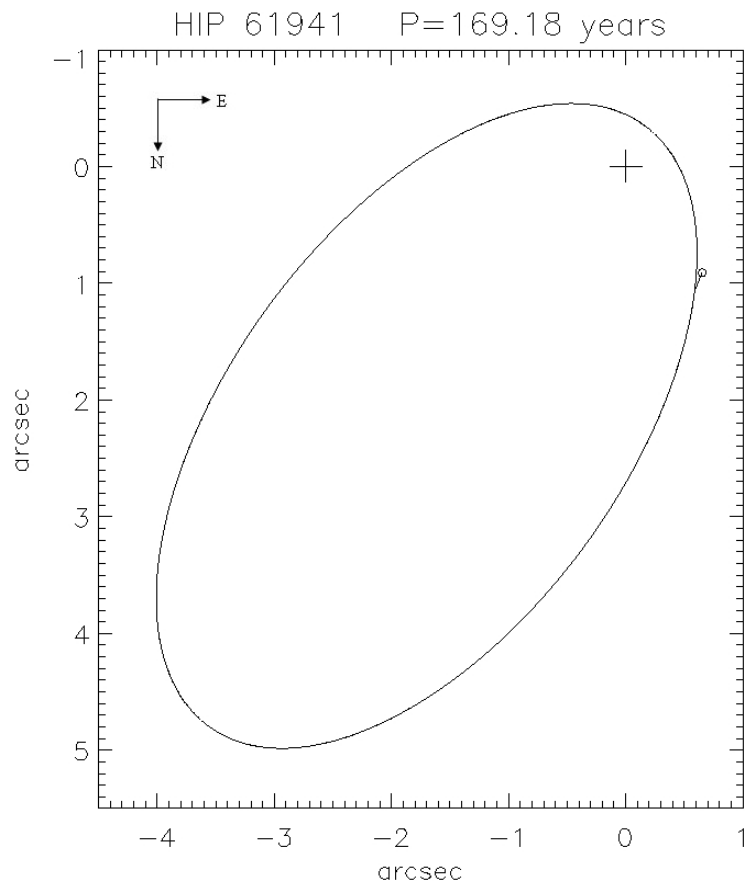
HIP 75695 P=10.27 years
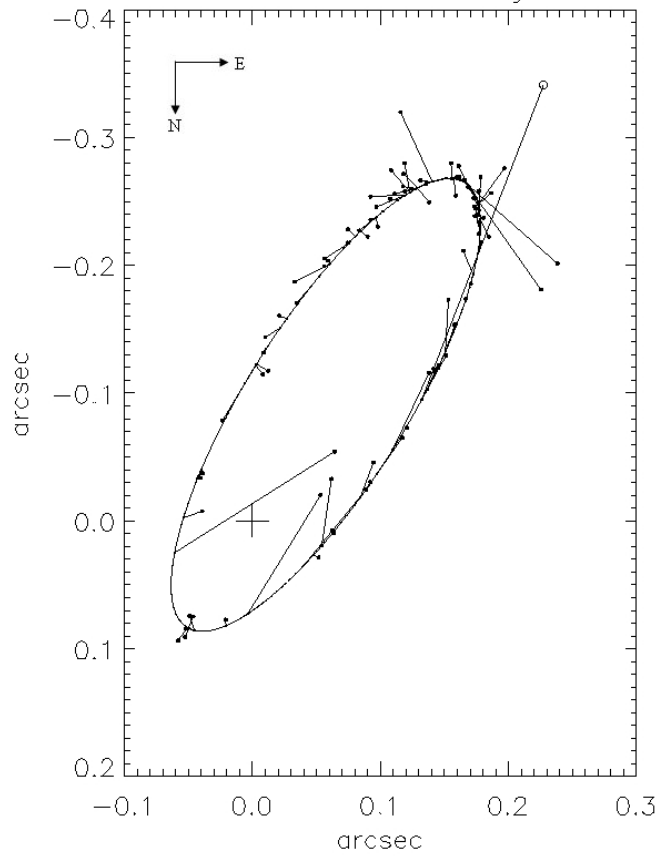
HIP 51233 P=38.62 years

HIP 64241   P=26.052 years

E
N

HIP 75312   P=41.556 years

E
N

30

HIP 76852   P=21.97 years

HIP 76952   P=92.94 years
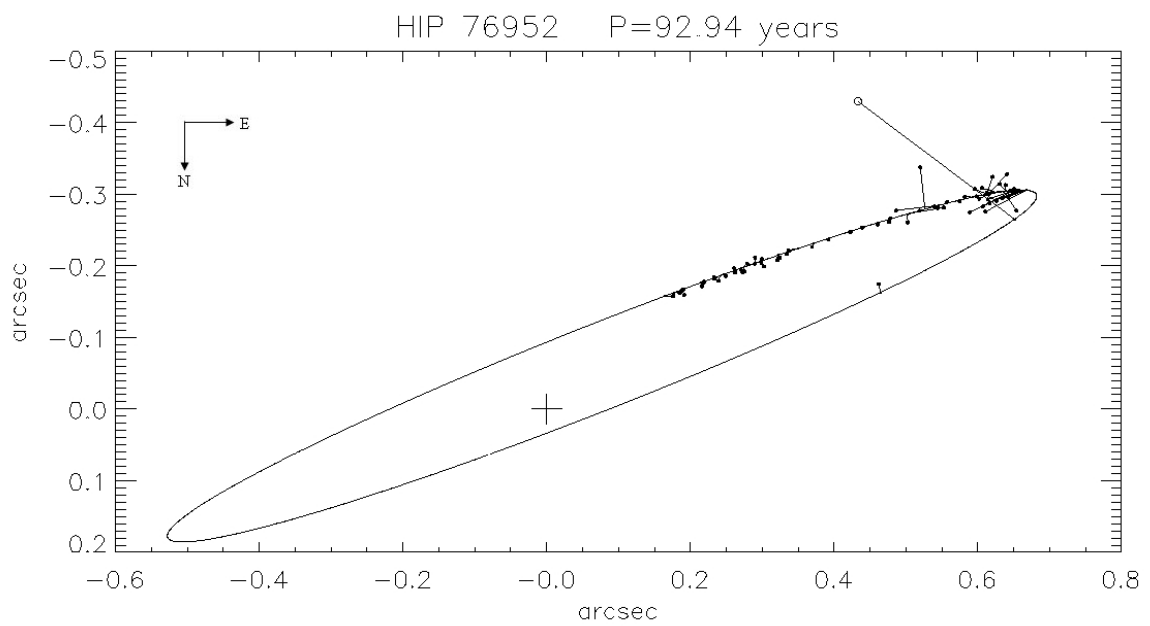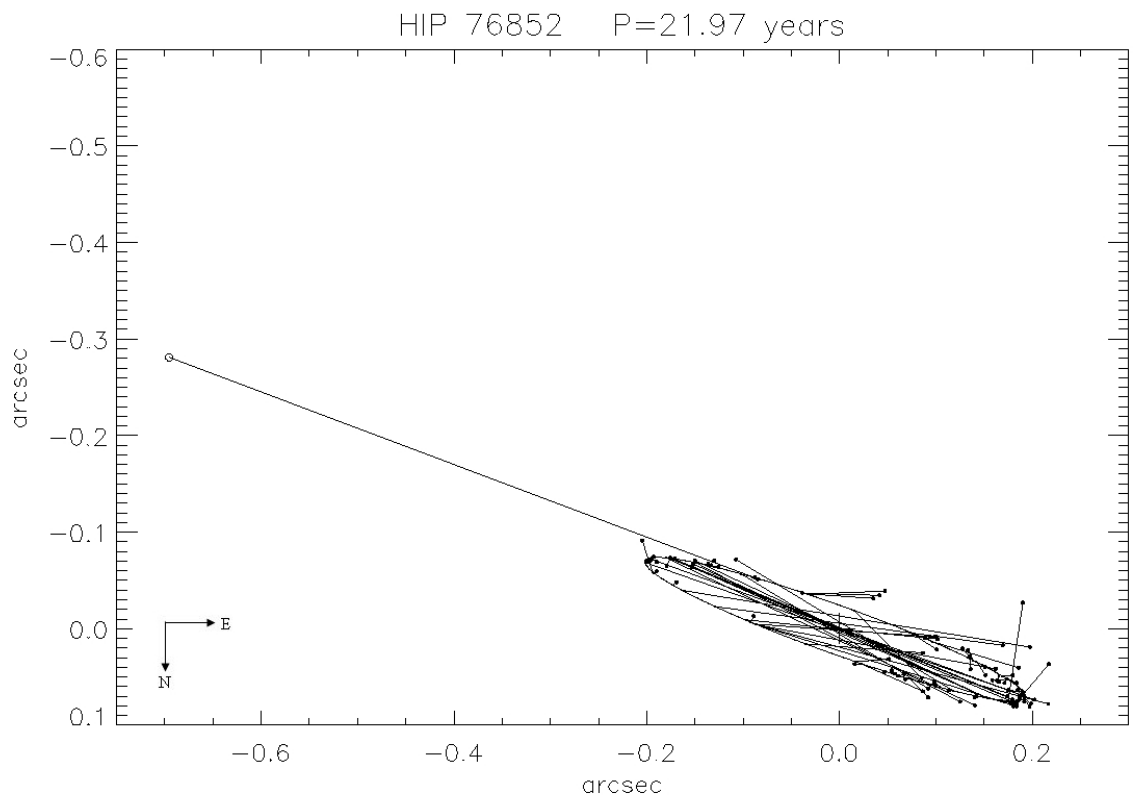
HIP 102531   P=3249 years

32
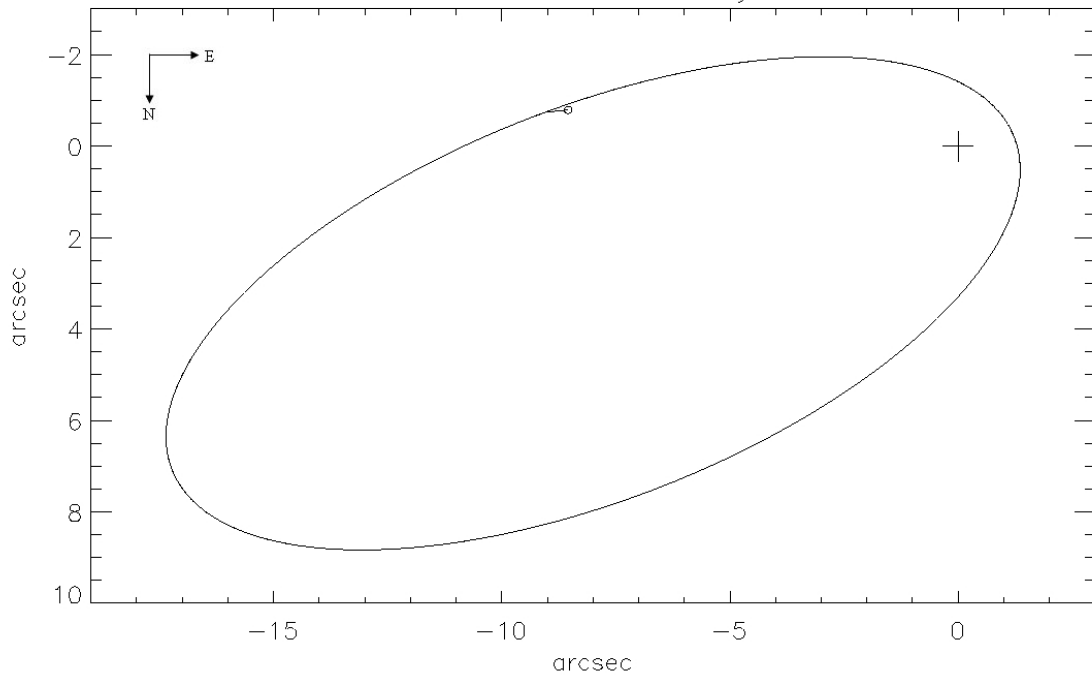
6 Discussion and Conclusion

In this speckle observation, we used the 14-inch Schmidt-Cassegrain telescope manufactured by Celestron. It is the type of telescopes whose primary mirror has mobile focusing pattern. After the telescope moves, the primary mirror also moves The synthetical focal-length will then changes. The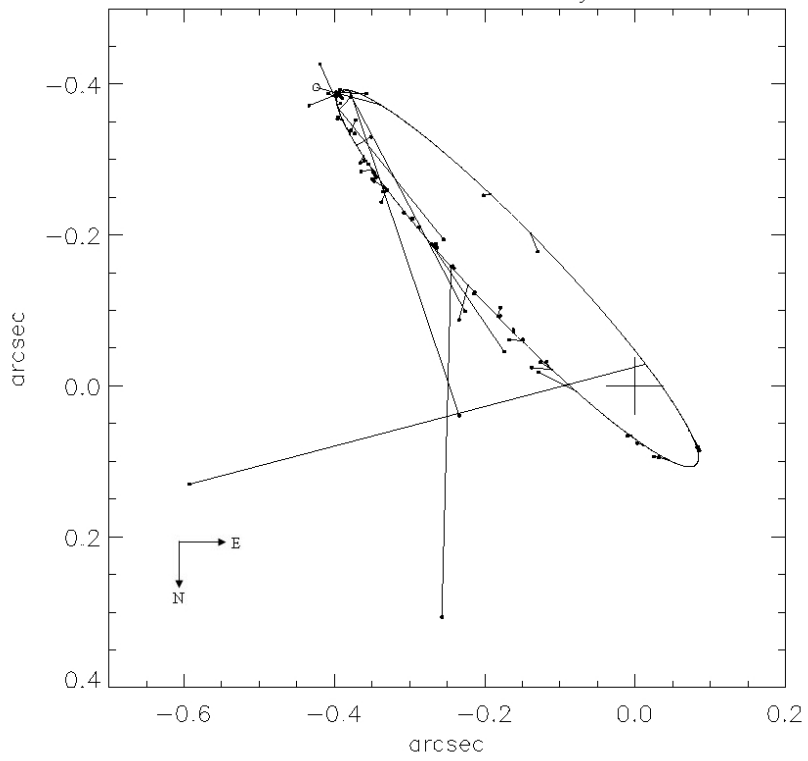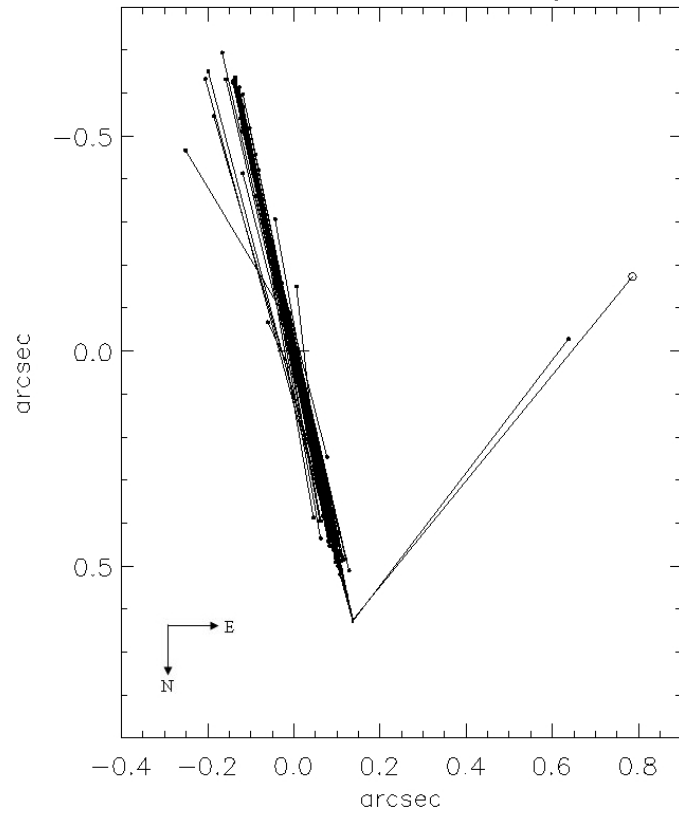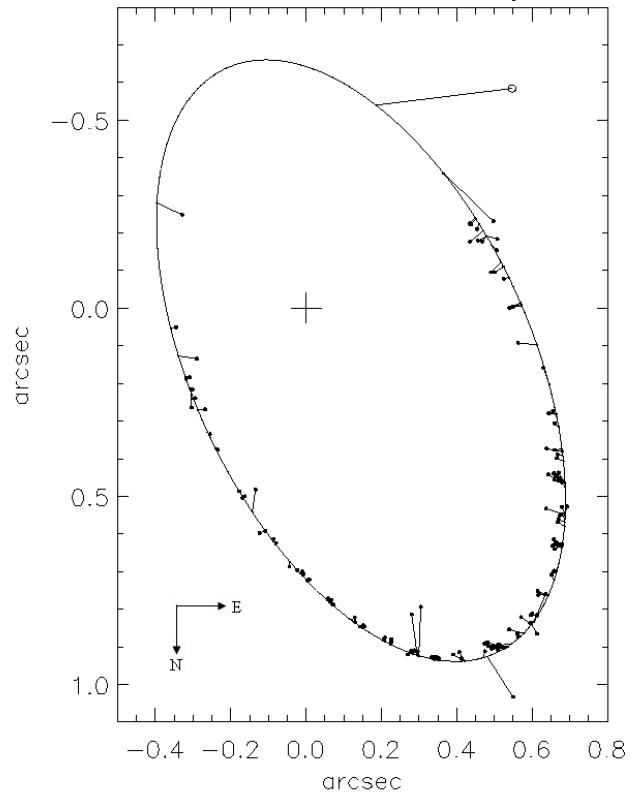refore, the focal length could be different in each observation. We measured the focal length with the double slit that also changed, and the error of the real focal length would increase. Therefore this type's telescope would not be suitable for the observations.

In the speckle observation, it is shown that a commercial camera CCD is suitable for speckle interferometry observation of a binary and to reach the diffraction limit of the small or moderate sized telescopes.

Speckle interferometry is one of the methods for most the telescopes to observe binaries with separations less than the seeing disk. Among the 22 binaries chosen for our 2009 program, the parameters of 13 binaries are determined. The magnitude limit of the primary star is brighter than 5 mag, the secondary is brighter than 6 mag. The limit of magnitude difference between primary and secondary stars is 2 mag ($\Delta m=2$). It is a pity that the primary star didn't reach 6th magnitude. However the small telescopes are able to resolve the binaries with angular separation larger than 0.3 arcsec.

In future, we will collect more data as possible as we can. In addition, the speckle observation of binary at NTNU will become routine program. We may use larger telescopes such as 1-m telescope (LOT) at Lulin Observatory. The telescope with a larger diameter can increase the light-gathering power and detect binary stars to 9th magnitude. Furthermore, we choose cooled CCD camera or 12bit CCD that may increase the limit of magnitude difference between primary and secondary stars less than 2 mag.

References

Texereau, 1962, L'Astronomie, 76, 159.

Labeyrie, A., 1970, Ap. J. 123, 123.

Michelson, A. A. and Pease, F. G., 1921, Ap. J., 53, 249.

Gezari, D. Y., Labeyrie, A., Stachnik, R. V., 1972, ApJ, 173, L1.

Labeyrie, A., Bonneau, D., Stachnik, R. V., Gezari, D. Y., 1974, AJ, 194, L147.

McAlister, H. A. 1976, PASP, 88, 317.

Bonneau, D., Foy, R., 1980, A&A, 86, no. 3, 295.

McAlister, H.A., 1981,A.J, 86,1397M.

Weigelt G. and Wirnitzer B., 1983, OPTICS LETTERS, 8, 7.

Wang, Yi-Ming, Qiu, Yao-Hui, Lürui-Ning, Qian, Ping, 1988, ChA&A., 12.141W.

McAlister, Harold A., Hartkopf, William I., Sowell, James R., Dombrowski, Edmund G., Franz, Otto G, 1989, AJ, 97, 510.

Hartkopf, W. I., McAlister, H. A., 1991, Astrophysics and Space Science, 177, no. 1-2, 161.

Germain, Marvin E., 1994, AAS, 26, 1314.

Lewis, J. P., 1995, "Fast Normalized Cross-Correlation," Industrial Light & Magic.

Nils Henning Turner, 1997, A Prototype Imager for the CHARA array, thesis.

Hartkopf, William., McAlister, Harold A., Mason, Brian D., ten Brummelaar Theo, Roberts, Lewis C., Jr., Turner, Nils H., Wilson, John W., 1997, A.J, 114,1639H.

Baraffe, I., Chabrier, G., Allard, F., & Hauschildt, P. H. 1998, A&A, 337, 403.

Horch, Elliott, Ninkov, Zoran, van Altena, William F., Meyer, Reed D., Girard, Terrence M., Timothy, J. Gethyn, 1999, A.J., 117,548H.

Scardia, M., Prieur, J.-L., Aristidi, E., Koechlin, L., 2000, ApJS, 131, 561.

Marchetti, E., Faraggiana, R., Bonifacio, P., 2001,A&A, 370,524.

Prieur, J.-L., Oblak, E., Lampens, P., Kurpinska-Winiarska, M., Aristidi, E., Koechlin, L., Ruymaekers, G., 2001A&A, 367,865P.

Rutkowski, Artur, Waniak, Waclaw, 2005, PASP, 117, 1362.

Muller, R. J., Cersosimo, J. C., Cotto, D., Rosado de Jesus, I., Centeno, D., Miranda-SanFeliz, V., Martinez, C., 2005, AAS, 207,1106M.

Scardia, M., Prieur, J.-L., Sala, M., Ghigo, M., Koechlin, L., Aristidi, E., Mazzoleni, F., 2005, MNRAS, 357,1255S.

Mason, Brian D., Hartkopf, William I., Wycoff, Gary L., Holdenried, Ellis R., 2006, AJ,

132, Issue 5,. 2219.

Brian D. Mason, Gary L. Wycoff, and William I. Hartkopf, 2006 Washington Double Star Catalog.<http://ad.usno.navy.mil/wds/>

William I. Hartkopf, Brian D. Mason, and Gary L. Wycoff, 2006 Fourth Interferometric Catalog.<http://ad.usno.navy.mil/wds/int4.html>

William I. Hartkopf and Brian D. Mason, 2006 Sixth Orbit Catalog. <http://ad.usno.navy.mil/wds/orb6.html>

Bagnuolo, William G., Jr., Taylor, Stuart F., McAlister, Harold A., ten Brummelaar, Theo, Gies, Douglas R., Ridgway, Stephen T., Sturmann, Judit, Sturmann, Laszlo, Turner, Nils H., Berger, David H., Gudehus, Donald, 2006, A.J, 131,2695B.

Yan Y.C., Fu H.H., 2007, Speckle Interferometry of Selected Binaries Using Philips

Docobo, J. A., Andrade, M., Tamazian, V. S., Costado, M. T., Lahulla, J. F., 2007, RMxAA, 43, 141.

Muller, Rafael J., Centeno, D. C., Rivera-Rivera, L. A., Morales, K., Ramos, K., Franco, E., 2007, AAS, 211,0388M.

Scardia, Marco, Argyle, Robert, Prieur, Jean-Louis, Pansecchi, Luigi, Basso, Stefano, Law, Nicholas, Mackay, Craig, 2007, IAUS, 240,558S.

Schlimmer, Joerg, 2007, JDSO, 3,131S.

Calloi, Roberto, 2008, JDSO, 4,111C.

Horch, Elliott, Anderson, L., DeSousa, M., van Altena, W. F., 2009, DDA, 40,1604H.

VirtualDubMod download from Avery Lee's VirtualDub,

http://sourceforge.net/projects/virtualdubmod/

Appendix

Appendix A　Specifications of Equipments

Cross section illustration of Celestron 14-inch
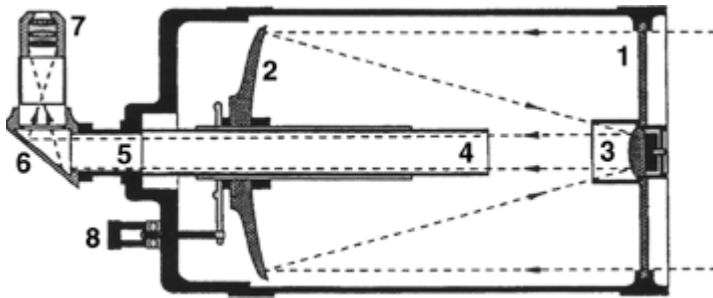
1. Light enters through the Corrector Lens
2. Primary Mirror
3. At the rear of the telescope tube forward to the Secondary Mirror.
4. Light is then reflected from the Secondary Mirror back through Primary Baffle Tube
5. beyond the Rear Cell
6. Illustration shows the Rear Cell with accessories attached: 90 degree Zenith Prism
7. (or Mirror) diagonal, and an Eyepiece
8. The Focus Control Knob

http://www.company7.com/celestron/products/sch13.html

Specifications of the Celestron 14" Schmidt-Cassegrain Telescope Optical System

Design	Schmidt-Cassegrain Catadioptric
Effective Aperture	14 inches, 355.6mm
Nominal Focal Length	154 inches, 3910mm
Nominal Focal Ratio	f11
"Fastar" Focus Focal Length	29.4 inches, 747mm
"Fastar" Focus Focal Ratio	f2.1
Primary Mirror	14.25" Diameter, f2.14, Radius 60" (1,524mm), Spherical of fine annealed Pyrex®
Secondary Mirror	3.5" (88.9mm) Diameter, Radius 17.6" (440mm), Amplification ratio 5.14, Spherical (final hand figuring yields a slight asphere) of fine annealed Pyrex®
Corrector	0.220" (6.4mm) thick parallel, aspheric Schmidt curve on R1 and Plano R2, of Soda Lime Float,

	Mgf2 AR coatings each side
Mirror Coatings	Celestron "Starbright®": 5 step multi layer
Central Obstruction	4.5" overall
Highest Useful Magnification	Approx. 840x
Lowest Typical Magnification	70x (0.68 degrees) with 2" 55mm Plossl (5.07mm Exit Pupil)
Resolution, Visual	Dawes Limit: 0.33 arc seconds
Stellar Magnitude Limit, Visual	About Magnitude 15
Resolution, Film	182 lines per mm at 4100nm
Image Scale (CCD or Film)	0.014 degrees per mm
Light Gathering Power	2581X Theoretical. Approx. 1940X actual over human eye (with 7mm entrance pupil)
Near Focus	Approx. 100 feet (30.5 meters)
Optical Tube Dimension	Length 30" (76cm), Diameter 16" (40.6cm)
Back Focus	14 inches from Apex of Primary Mirror
Optimum Back Focus	Approx. 4 inches; with f6.3 Reducer/Corrector 4" from rear of Reducer

http://www.company7.com/celestron/products/sch13.html

Specifications of Titan mount system

R.A. Gear Wheel:	6.7500", 270 tooth 7075 T35 aluminum
DEC. Gear Wheel:	6.7500", 270 tooth 7075 T35 aluminum
DEC. and R.A. Worm gear:	440C Stainless (54 Rockwell hardness)
Worm Gear Support:	Dual supported ball bearings
Preload:	Adjustable
Worm Gear Period:	5 minutes 20 seconds
R.A. Axis Needle Thrust Bearings:	5.062" Dia. needle thrust, 3.500 ball
DEC. Axis Needle Thrust Bearings:	5.062" Dia. needle thrust, 3.500 ball
DEC. and R.A. Clutches:	6.0" Slip clutch, variable friction, one knob ea. axis
Latitude Working Range:	12 to 70 degrees
Azimuth adjustment range:	+ or - 10 degrees
Dovetail Saddle Plate:	1.00 x 6.00 x 8.00" Split Saddle
Dovetail Male Plates:	D Series
Mass of Equatorial Mount Head	Approximately 84 lbs.
Load Capacity:	Approximately 150 lbs.

http://www.company7.com/losmandy/titan.html

Specifications of 16 inch (0.41 meter) f/9 Ritchey-Chrétien Optical System

Delivery Status	45-60 Days Upon Receipt of Optics
Focal Length	4115mm
Overall Length/Diameter	46"/16"
Total Weight*	93 pounds
System	16" f/9
Primary Focal Length	48"
Back Focus	14"
Secondary Amplification	2.85X
Radius of Field Curvature	17.67"
Secondary Size	6.0"
Primary Hole	3.75 - 4.0"

16 inch f/9 ION Milled Ritchey-Chrétien optics by ARIES INSTRUMENTS Co, Kherson, Ukraine Ritchey-Chrétien Zero Expansion Astro-Sitall Optics certified to at least 1/8 wave P-V and 1/40th wave RMS.

Supporting Fringe Analysis and interferometric data supplied with each optical set.

RCOS 18-point Flotation Mirror Cell.

Enhanced Aluminum (SiO2/TiO2) overcoat - 96.9% reflectivity.

Low expansion, light weight Carbon Fiber Truss for superior performance and stability.

6061 Aluminum components - All CNC Machined.

Precision Secondary Mirror Focuser.

2-Stage Primary mirror baffle with internal knife-edge light stops.

Conical Secondary light baffle.

6061 Aluminum Mounting Rings - CNC Machined.

Active Cooling.

RCOS "Focus and Forget" Technology.

Shipped fully assembled, collimated, and ready to use.

RCOS Custom CNC Machined "light weight" Losmandy compatible dovetail plates - top and bottom with matching Paramount VersaPlate hole pattern, allows dovetail mounting plate to be bolted to VersaPlate once scope is balanced.

Losmandy RDF-90 Finder Scope 3-point mounting bracket.

CNC machined dust cover over primary mirror.

Specification of detailing all parameters of the DMK 31AF03.AS

Camera Parameter	Parameter Value
Product Code	DMK 31AF03.AS
Type	monochrome FireWire camera without IR cut filter
Connection	FireWire
Manufacturer	The Imaging Source
Sensor	CCD
Type	progressive scan
Sensor specification	SONY ICX204al
Format	1/3"
Resolution	1024 x 768 pixel
Dynamic range	8 bit
Exposure time	1/10000 s to 60 minutes
Gain	0 dB to 36 dB
FPS @ Max resolution	30 fps
Video formats @ Frame rate	1024 x 768, Y800 @ 30, 15, 7.5, 3.75 fps
Lens mount	C/CS mount
Supply voltage	8 V to 30 V via the cable
Current consumption	approx 200 mA @ 12 VDC
Dimensions (H x W x L)	50.6 mm x 50.6 mm x 50 mm
Mass	265 g
Max. temperature (operation)	-5 °C to 45 °C
Max. temperature (storage)	-20 °C to 60 °C
Max. humidity (operation)	20 % to 80 %
Max. humidity (storage)	20 % to 95 %

http://www.astronomycameras.com/en/products/firewire-cameras/mono/dmk31af03as/

Interline CCD image sensor

Image size	Diagonal 6mm (Type 1/3)
Total number of pixels	1077 (H) ₓ 788 (V) approx. 850K pixels
Number of effective pixels	1034 (H) ₓ 779 (V) approx. 800K pixels
Number of active pixels	1024 (H) ₓ 768 (V) approx. 790K pixels (diagonal 5.952mm)
Chip size	5.80mm (H) ₓ 4.92mm (V)
Unit cell size	4.65μm (H) ₓ 4.65μm (V)
Optical black	Horizontal (H) direction: Front 3 pixels, rear 40 pixels
	Vertical (V) direction: Front 7 pixels, rear 2 pixels
Number of dummy bits	Horizontal 29
	Vertical 1
Substrate material	Silicon

http://www.theimagingsource.com/downloads/icx204al.en_US.pdf

Appendix B   Orbital elements of targets from 6th Catalog of Orbits of Visual Binary Stars (Hartkopf & Brian 2006),

WDS	NAME	HIP	V1	V2	P	a	i	Ω	T	E	ω	LAST	REF
05167+4600	ANJ 1Aa	24608	0.08	0.18	104.022	56.47	137.18	40.8	47528.45	0	0	1992	MkT1994
05407-0157	STF 774Aa,B	26727	1.88	3.7	1508.6	2.728	72	155.5	2070.6	0.07	47.3	1955	Hop1967
07346+3153	STF1110AB	36850	1.93	2.97	444.95	6.593	114.61	41.46	1960.1	0.323	253.31	1985	Doc1985c
08468+0625	SP 1AB	43109	3.8	5.3	15.0507	0.2547	50.01	107.99	1991.247	0.6558	266.1		Hrt1996a
09521+5404	STT 208	48402	5.28	5.39	105.4	0.349	24.5	130.3	1987.4	0.45	35		Hei1996c
10279+3642	HU 879	51233	4.62	6.04	38.62	0.363	79.1	41.5	1999.15	0.668	29.8	1997	Msn2001c
11182+3132	STF1523AB	55203	4.33	4.8	59.878	2.536	122.13	101.85	1935.195	0.398	127.94	1994	Msn1995
12417-0127	STF1670AB	61941	3.48	3.53	169.1	3.643	149.4	35.3	2005.51	0.882	255	2006	Sca2006b
13100+1732	STF1728AB	64241	4.85	5.53	26.052	0.67633	90.098	192.235	1989.205	0.5083	280.121	2005	WSI2006b
14411+1344	STF1865AB	71795	4.46	4.55	123.44	0.595	142	129.99	1897.59	0.957	1.47	1953	Wrz1956a
15232+3017	STF1937AB	75312	5.64	5.95	41.556	0.86821	57.973	203.17	1975.464	0.2742	38.83	2005	WSI2006b
15278+2906	JEF 1	75695	3.68	5.2	10.27	0.205	111.1	148.2	1980.506	0.524	181.3	1983	Tok1984
15416+1940	HU 580AB	76852	5.35	5.22	21.97	0.21	83.2	70.3	2006.98	0.084	76.3	2001	Doc2007d
15427+2618	STF1967	76952	4.04	5.6	92.94	0.7353	94.7	111.25	1931.66	0.484	105.24		Hrt1989
15496-0326	CHR 259	77516	3.75	5.39	36	0.37	103	296	1988.9	0.4	308		Gon2003
17146+1423	STF2140Aa-B	84345	3.48	5.4	3600	4.68	155.8	119.6	1835	0	0	1970	Baz1978
18055+0230	STF2272AB	88601	4.22	6.2	88.38	4.554	121.16	302.12	1895.94	0.4992	14		Pbx2000b
19307+2758	MCA 55Aac	95947	3.37	5.16	96.84	0.586	118	98.8	2010.27	0.719	77.2	1997	Hrt1999b
19474+1832	BLA 6	97365	4.32	4.95	10.11	0.051	140	170.2	1979.93	0.44	257.7		Eat1995
20375+1436	BU 151AB	101769	4.11	5.02	26.65	0.443	62.1	177.9	1962.87	0.355	348.8		Alz1998a
20467+1607	STF2727	102531	4.36	5.03	3249	10.22	148.78	88.06	2305	0.88	331.16	1993	Hle1994
22288-0001	STF2909	110960	4.34	4.49	587.18	3.847	138.2	129.8	1973.39	0.396	255.9	2001	Ole2004a

Appendix C　Young's double slits with C-14

For C-14, the images of interferometric pattern of the double slits with different separation of 12 cm, 14 cm, 16 cm, 18 cm, and 20 cm are shown in Fig. 4.1, and the intervals of interference pattern, Δy are 26.79, 23.35, 21.35, 19.22, and 17.25 pixels.

d (mm)	120	140	160	180	200
Δy (pixel)	26.79	23.35	21.35	19.22	17.25
α ($''$/pixel)	0.0327	0.0322	0.0308	0.0304	0.0305

The scale, $\alpha = 0.0328 \pm 0.00106$ $''$/pixel for $\lambda = 0.00051$ mm.

Fig. C.1 The interval of the double slits set in front of C-14. For example, the left image is 16cm of the interval of the double slits.

Appendix D   Plot the binary orbit in terms of orbital elements

When we look up to the sky, all of stars look like inlays in a plane. In fact, we see that is the image with projecting in a plane, rather than three dimensional structure. The real orbit of binary system can be reconstructed by the seven orbital elements.

The orbital elements are used for calculating the position of secondary via primary at the specific time. In celestial mechanics, the motion of binary is generally considered in classical two-body problem, and these seven elements can be calculated from the solution for the equation of motion of two-body. Usually, the orbital elements separate to two types, three geometric elements and four dynamical elements.

The relation between orbit of a binary and three geometric elements is shown on the Fig. C.1.
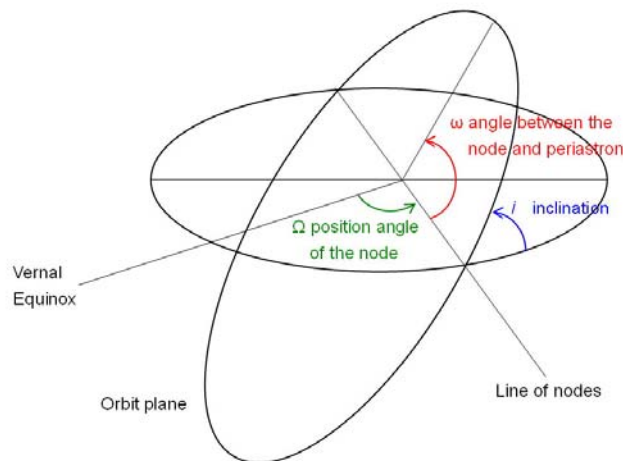
Fig. D.1 Geometric elements

Geometric elements

i	inclination of orbital plane
Ω	position angle of the node line
ω	angle between the node line and periastron

Dynamical elements

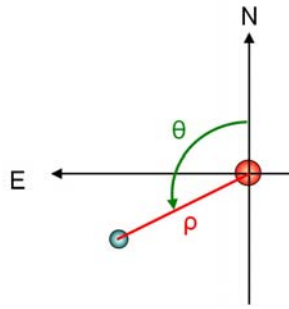|	
P	the period in years
E	Eccentricity anomaly
a	semi-major axis
T	time of periastron passage

Fig. D.2 Angular separation (ρ) and position angle (θ)

In order to know the orbit at the sky plane, the Euler angle transformation and the orbital elements are used to calculate the position of secondary via prinary. The Euler angles was developed by Leonhard Euler to describe a body in the three dimensional Euclidean space.

The coordinate of secondary via primary, x and y, are calculated from the observed angular separation (ρ) and position angle (θ) at time of t in the following formula,

$$x = \rho \cos \theta \quad \text{and} \quad y = \rho \sin \theta.$$

The other hand, x and y can be determined in terms of Thiele-Innes elements, A, B, F, G, and X, Y.

$$x = AX + FY,$$
$$y = BX + GY.$$

The Thiele-Innes elements are calculated with the geometrical elements, a, ω, Ω ,and i according to the following formula.

$$A = a (\quad \cos \omega \cos \Omega - \sin \omega \sin \Omega \cos i),$$
$$B = a (\quad \cos \omega \sin \Omega + \sin \omega \cos \Omega \cos i),$$
$$F = a (- \sin \omega \cos \Omega - \cos \omega \sin \Omega \cos i),$$
$$G = a (- \sin \omega \sin \Omega + \cos \omega \cos \Omega \cos i).$$

And X and Y can be calculated:

$$X = \cos E - e,$$
$$Y = (1 - e^2)^{1/2} \sin E,$$

where the value of E is from 0 to 2pi, responding the total orbital period.

The coordinates, x and y, are calculated from the Thiele-Innes elements, X, and Y, and the orbit of binary can be plotted.

- (O-C) in orbit of binary

In fact, the value of E can be calculated by Kepler's equation if the observed time of t, period of P, and the time of periastron passage of T are known.

$$E - e \sin E = 360(t - T)/P,$$

where P is the period in years.

The auxiliary circle of an ellipse is shown the Fig. C.3, and its origin, **o**, is the center of the ellipse with a radius of semi-major axis. When the secondary of binary move to the position, **P,** on the ellipse orbit, the eccentric anomaly (**E**) is defined as an angle shown in Fig. C.3 where line $\overline{Qx}$ is perpendicular to major-axis, and it intersect with major-axis at **x** and intersect with the auxiliary circle at **x**. That means, the eccentric anomaly (**E**) is the angle Q-o-**x**.
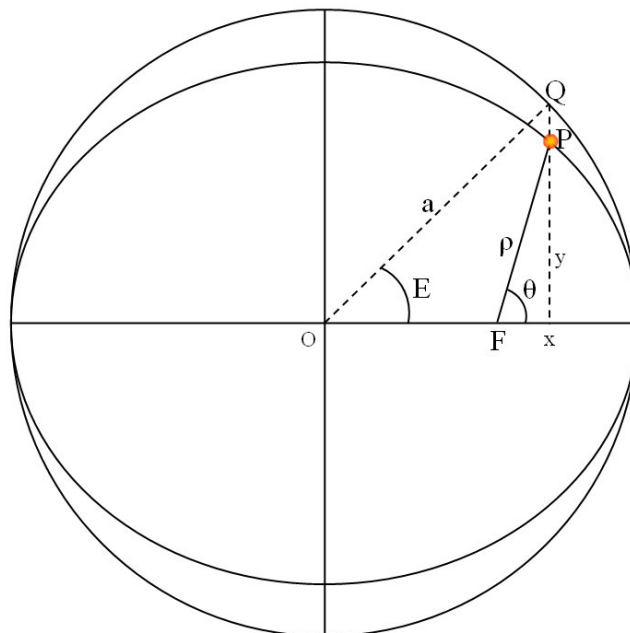
Fig. D.3 Eccentric anomaly
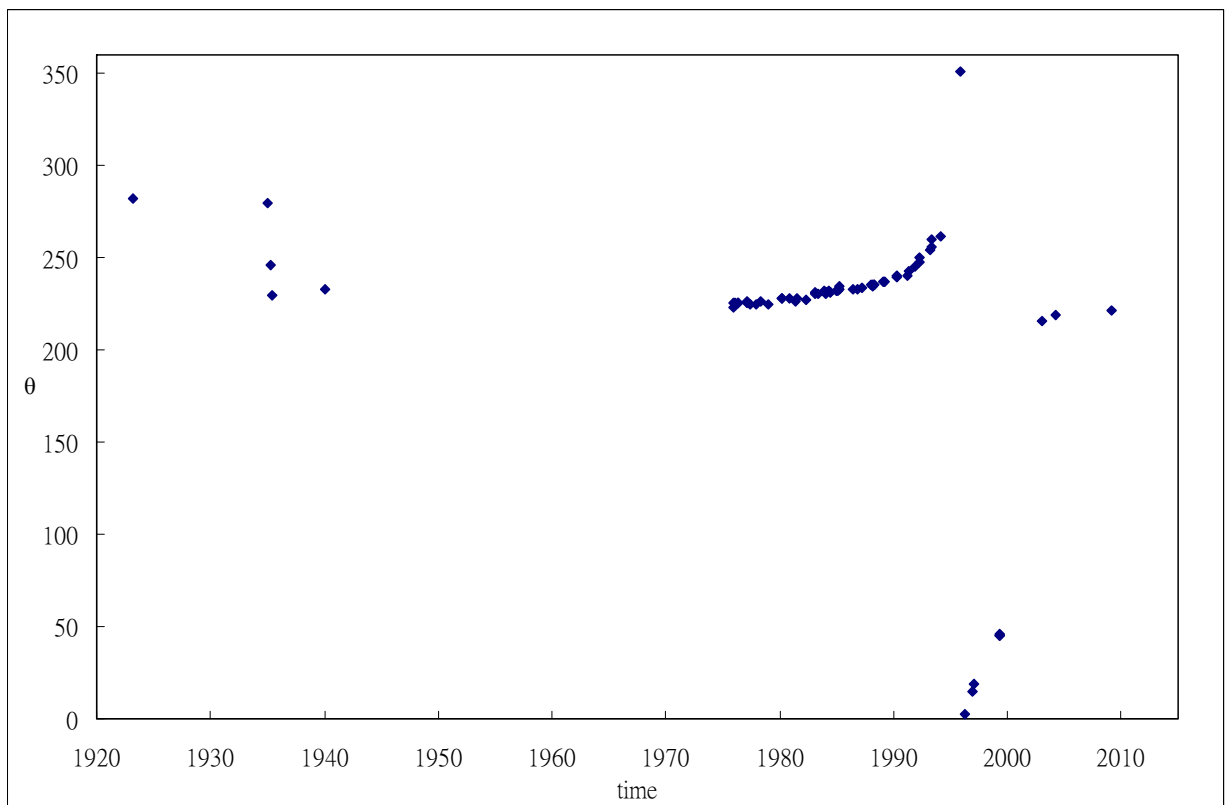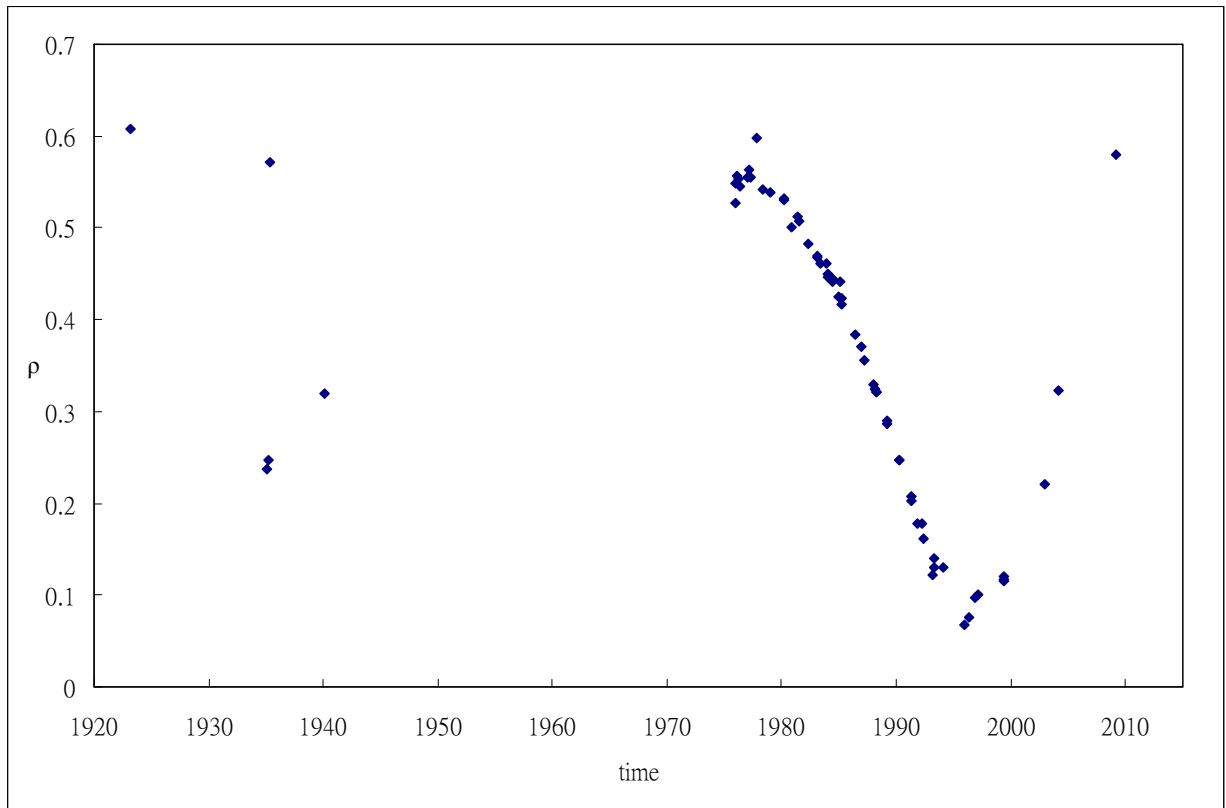
$$\rho = a\,(\,1 - e \cos E\,)$$

46

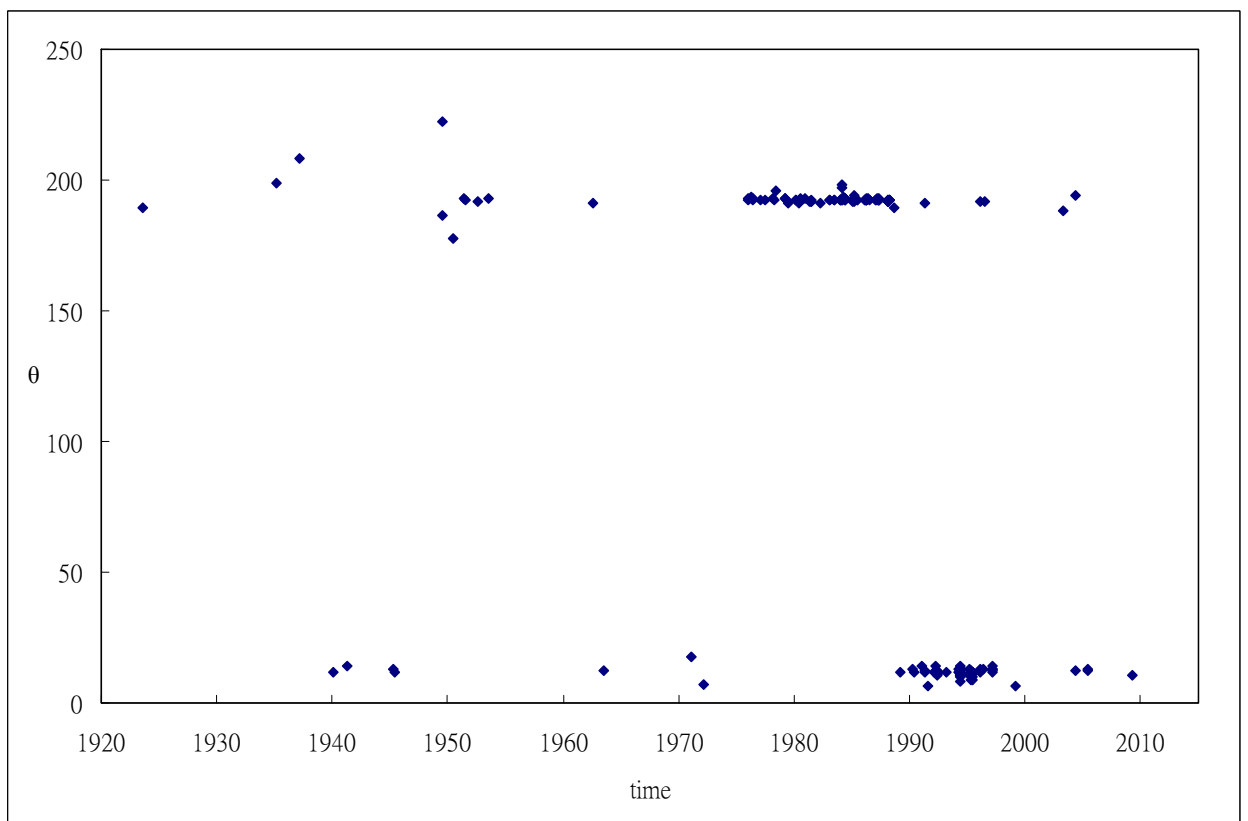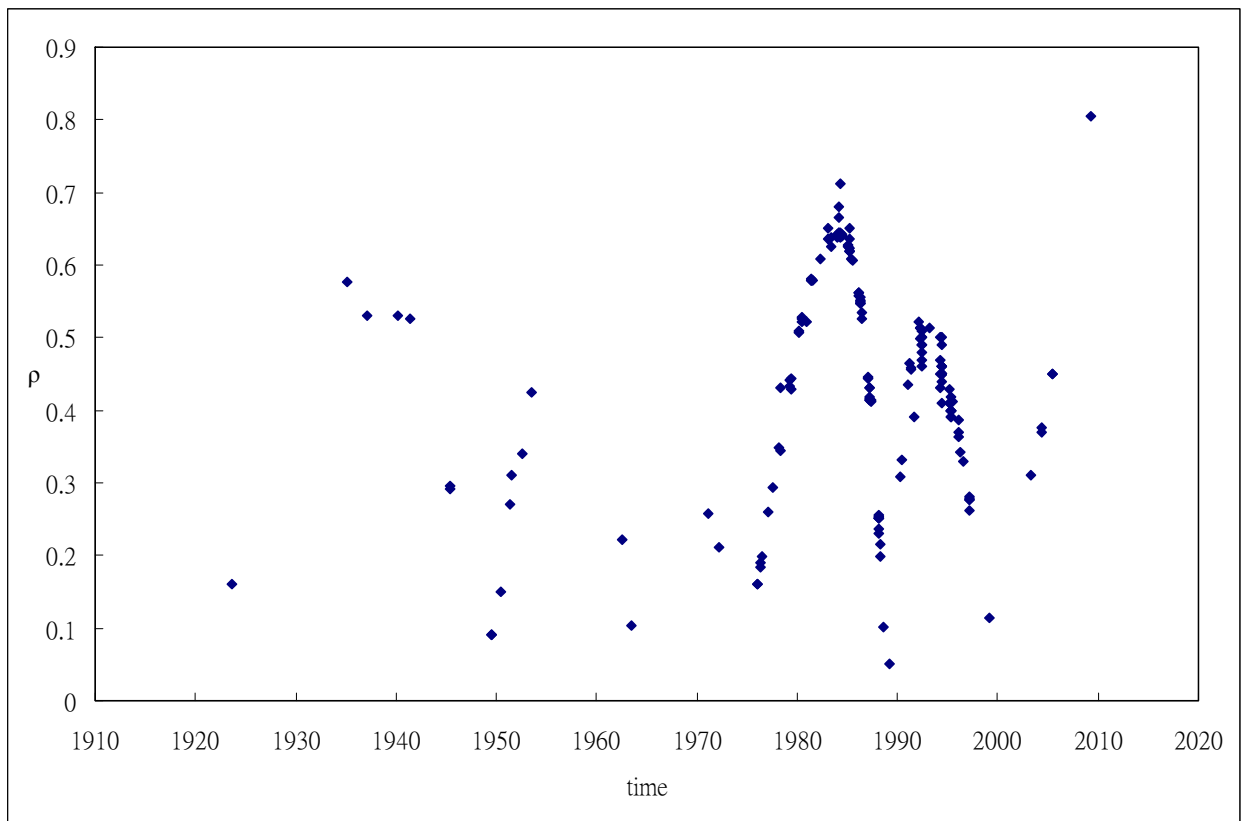# Appendix E   ρ and θ of the targets from WDS 2006.5 version the Fourth Catalog of Interferometric Measurements of Binary Stars.
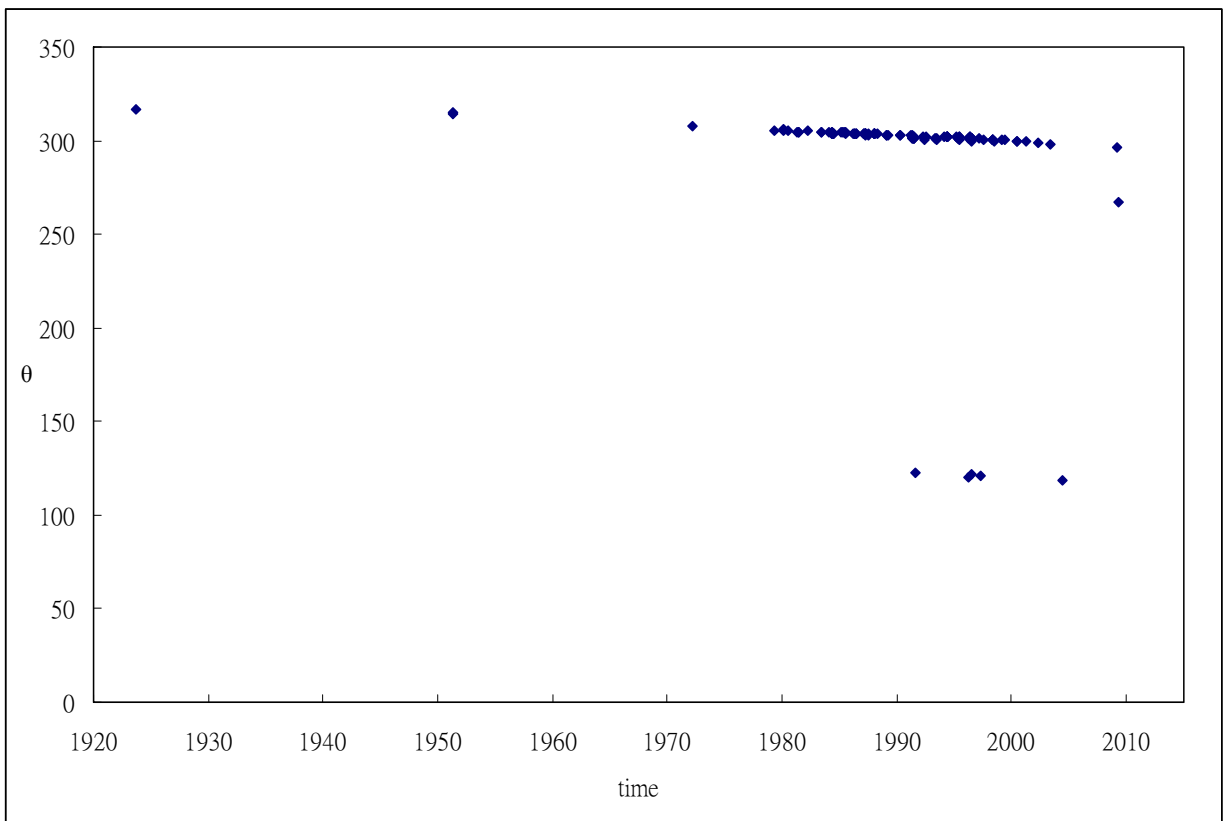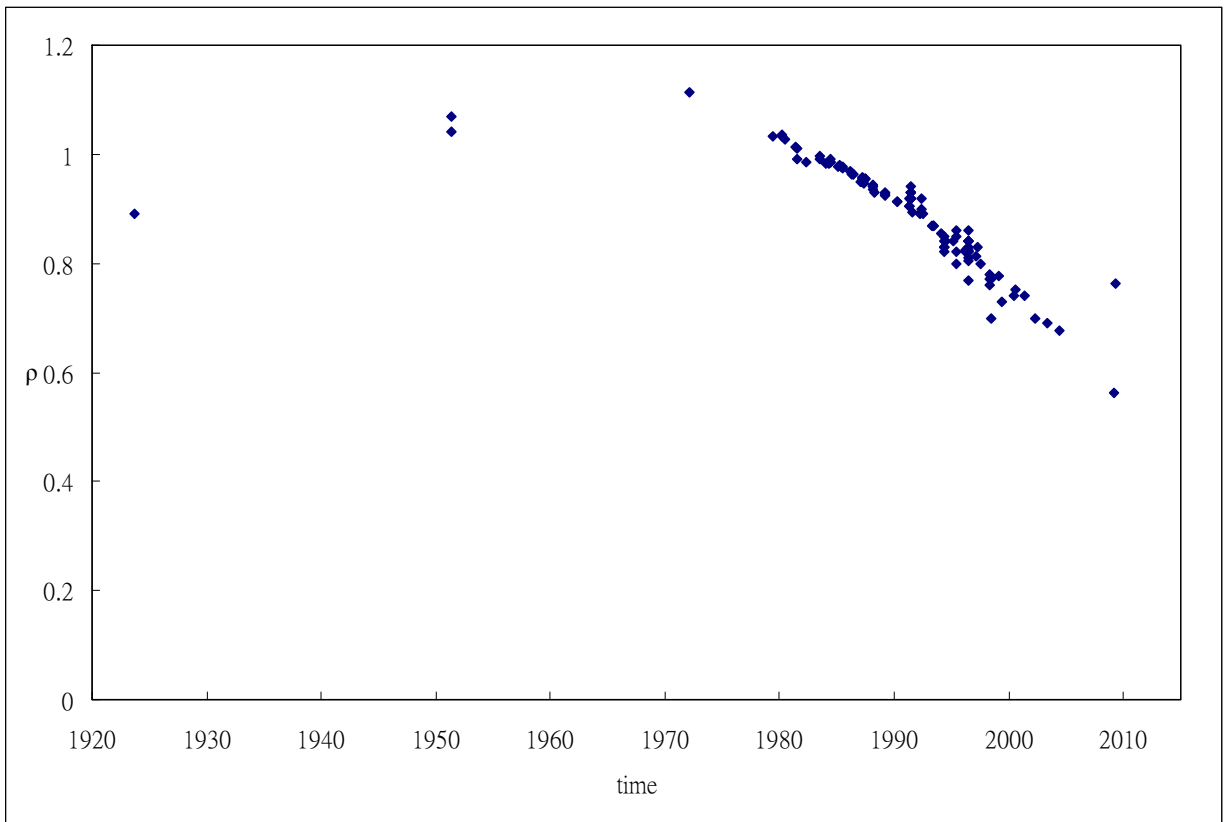
HIP 43109

HIP 51233

HIP 64241

49
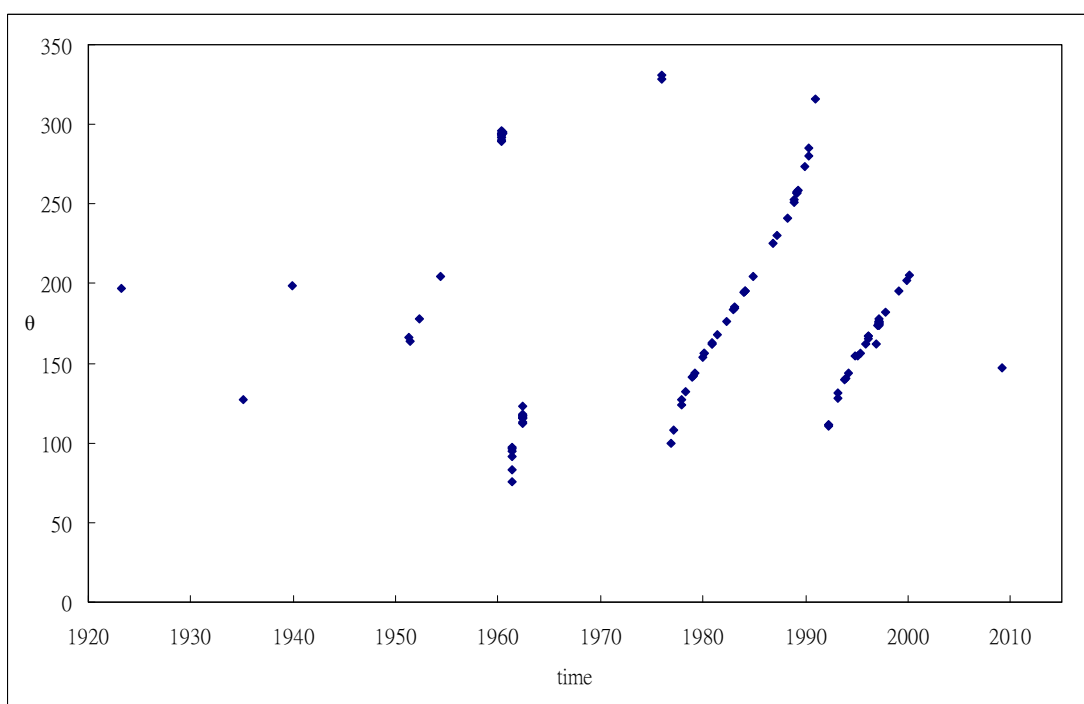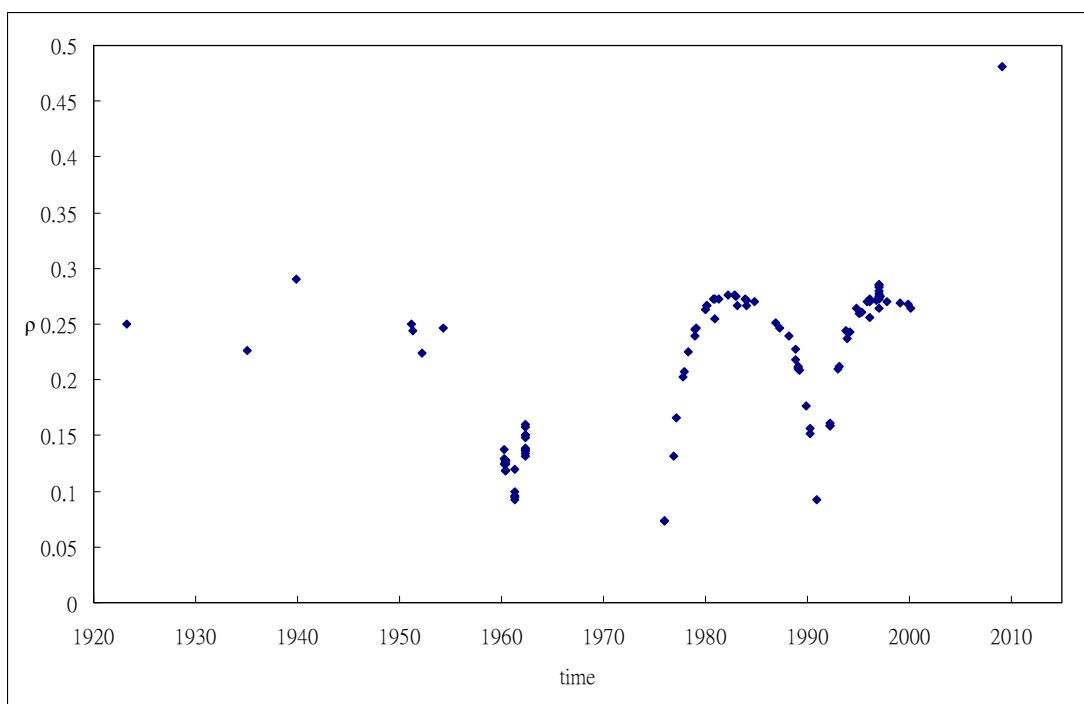
HIP 71795

HIP 75312
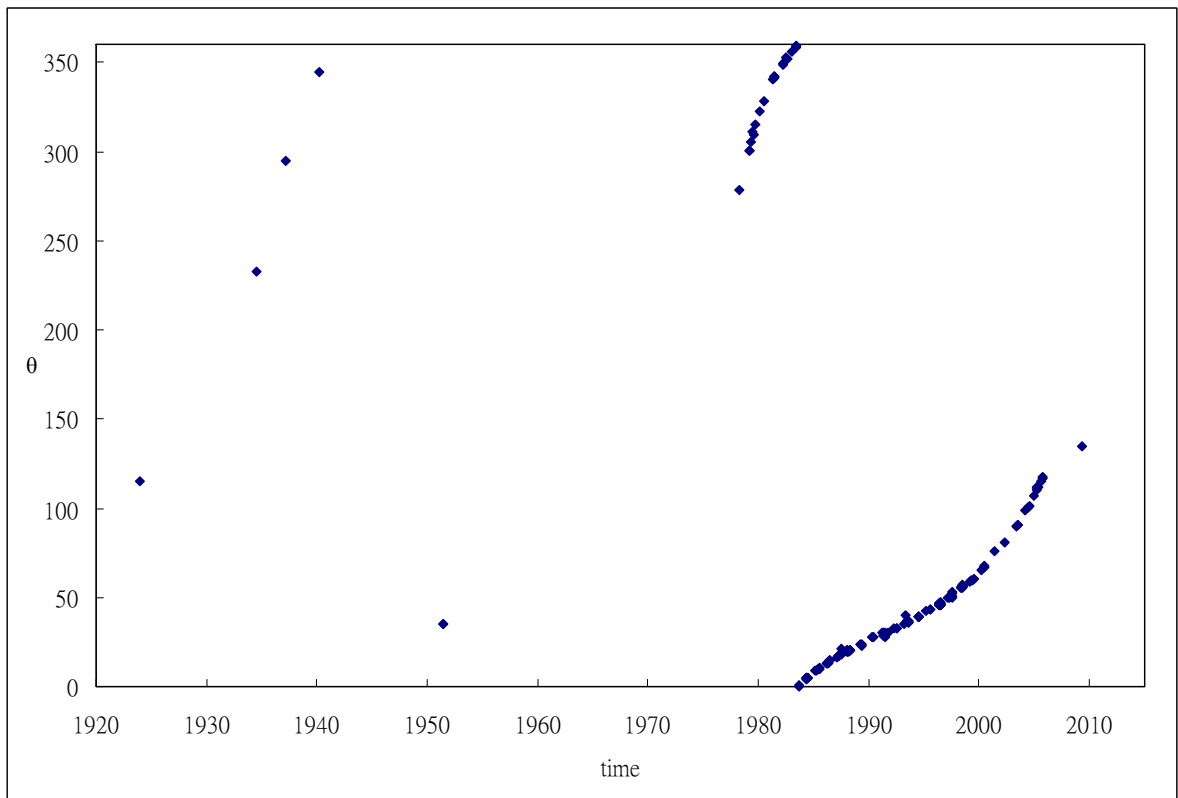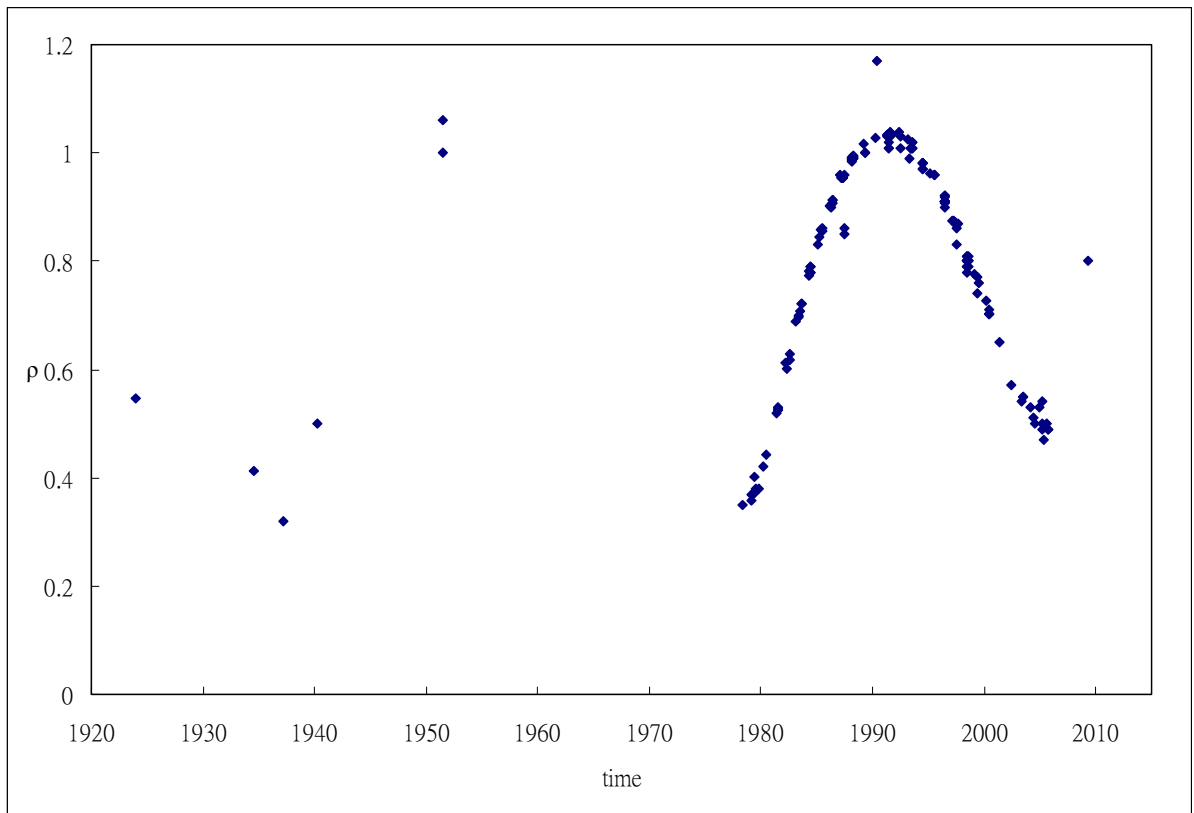
HIP 75695

HIP 76852

HIP 76952

54
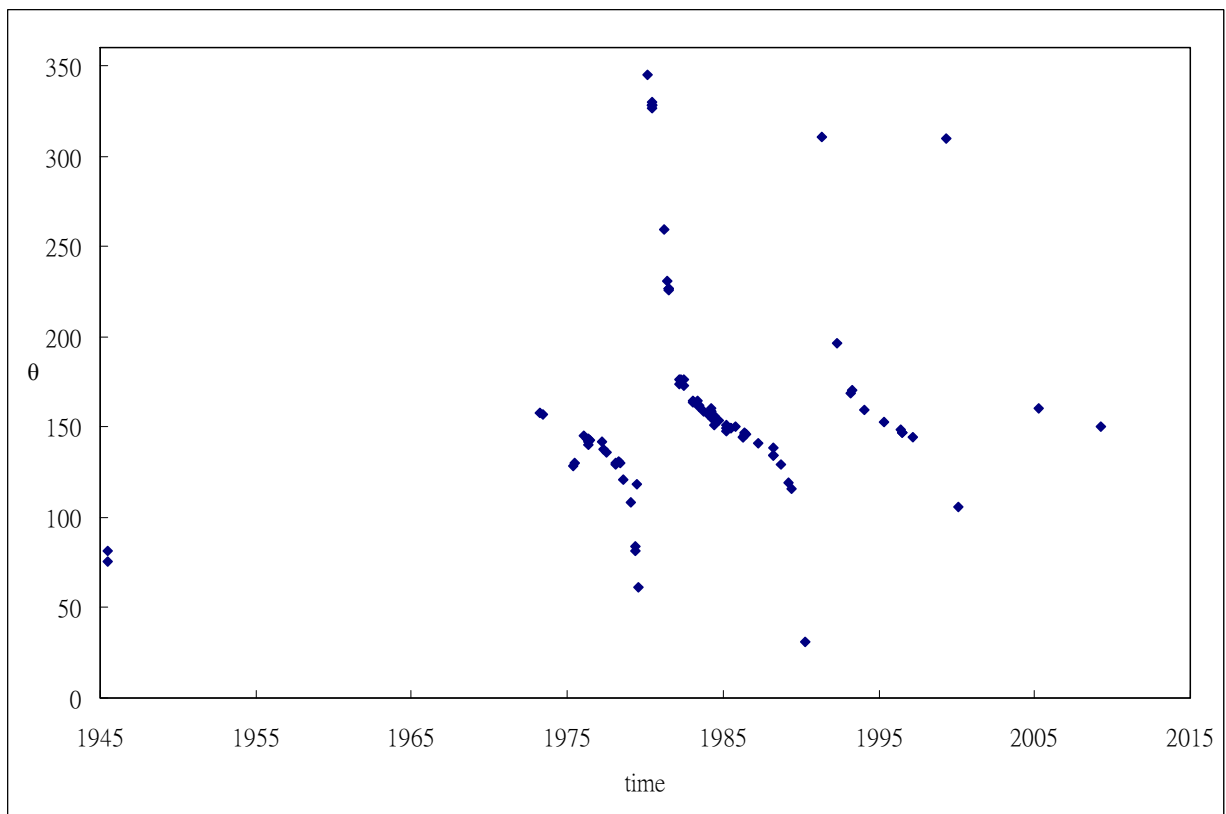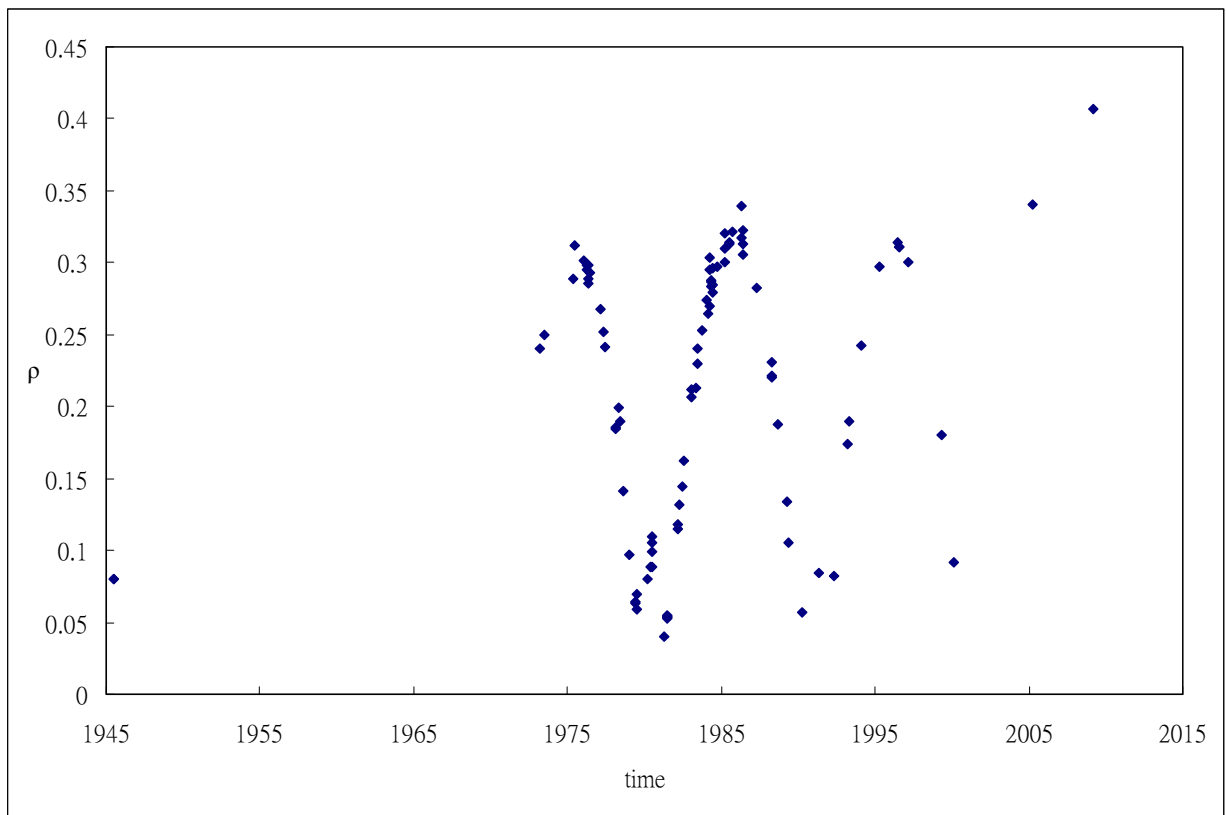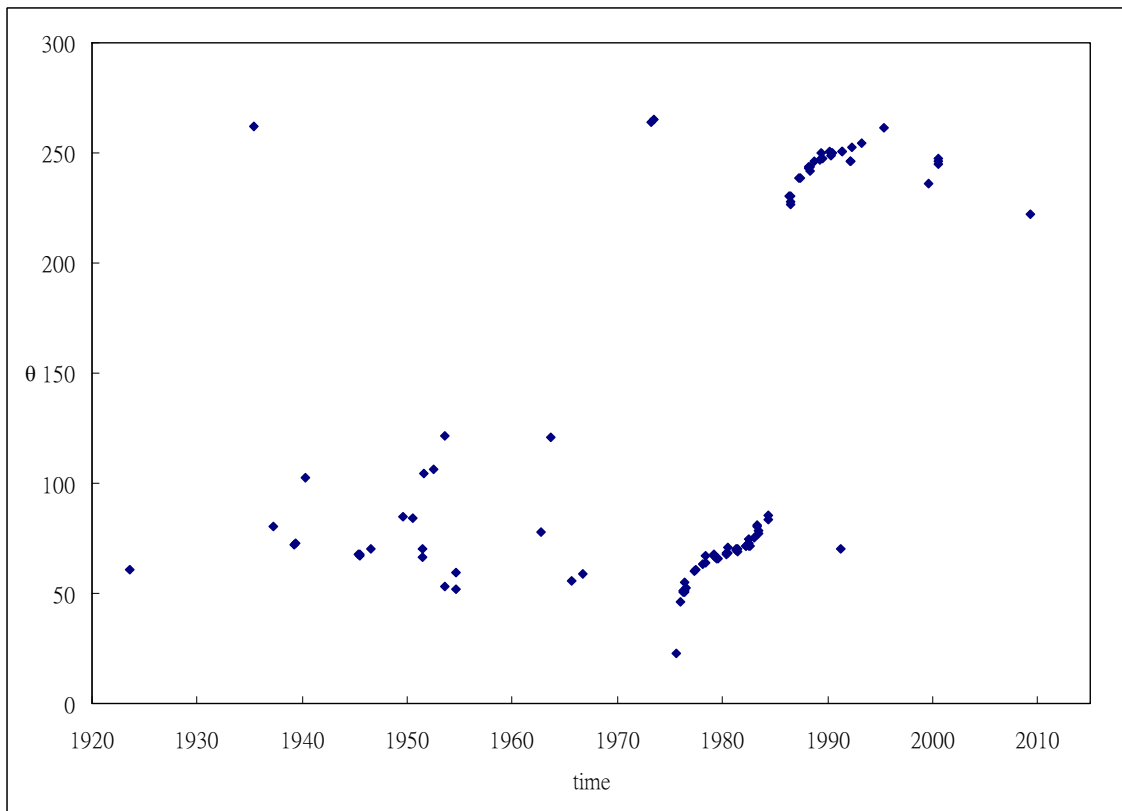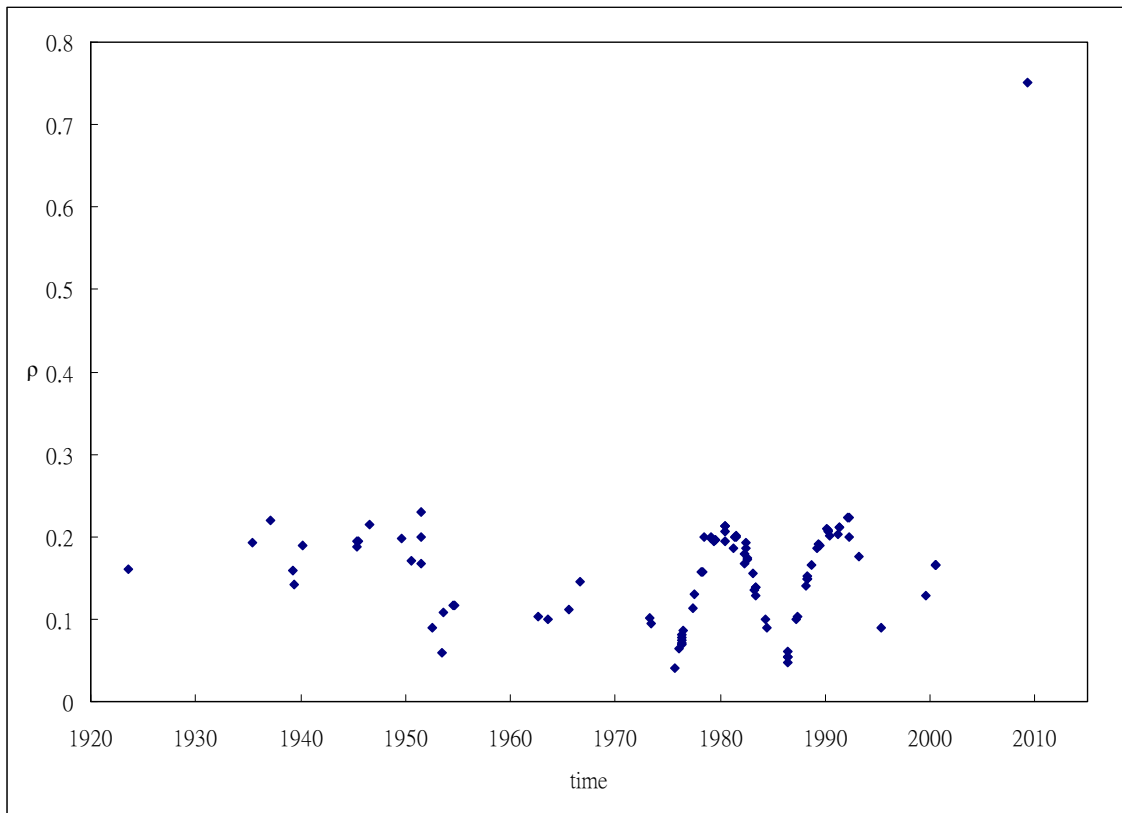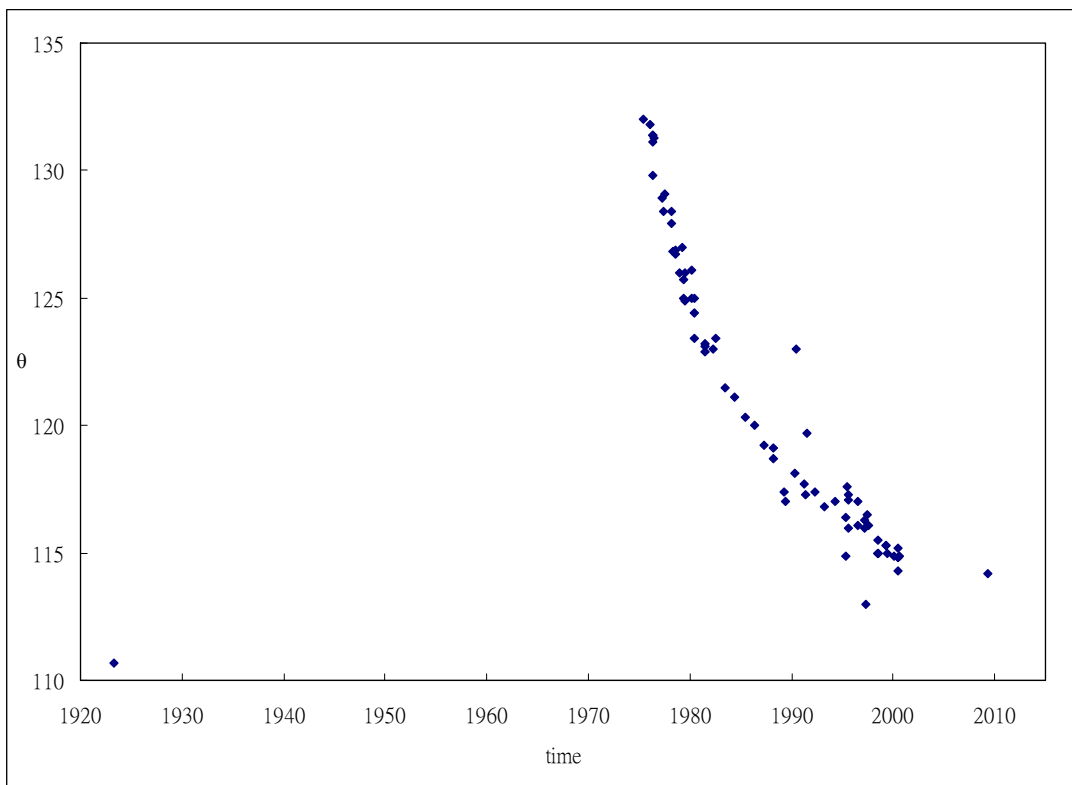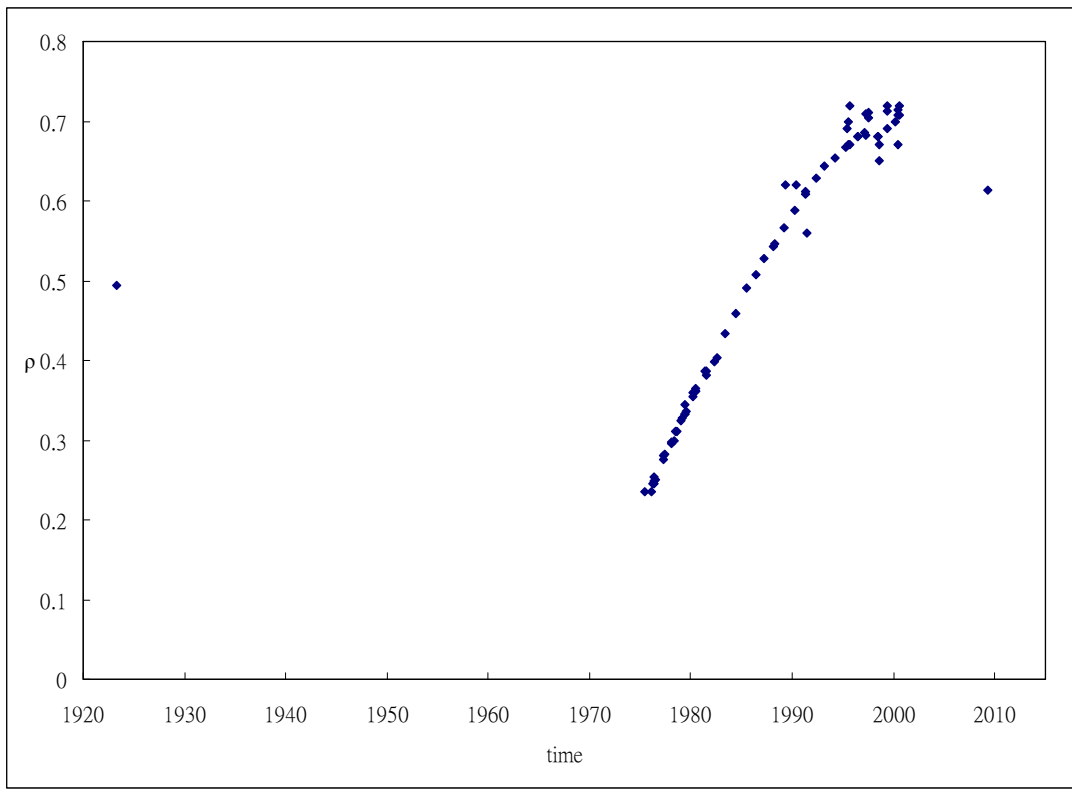
Appendix F IDL Source code of data reduction

```
pro hip64241

close,1
erase

img0=fltarr(300,300)
img0=0
sum=img0

openr,1,'D:\astro\data\20090317\hip64241\hip64241good.txt'
ii=48
s = strarr(ii)
readf,6,s

for in=0,ii-1 do begin
  figPath='D:\astro\data\20090317\hip64241\trans\'
  file = figPath + s(in)
  z = READ_BMP(file,R,G,B,ihdr,/RGB)
  image=fltarr(300,300)

;------- set small size and subtraction noise --------
    for ii=0,299 do begin
      for jj=0,299 do begin
        ixn=300+ii
        iyn=300+jj
        img=z(ixn,iyn)
        if img le 65 then z(ixn,iyn)=0
        image(ii,jj)=z(ixn,iyn)
      endfor
    endfor

;------------- fft ------------------------------
  f = shift(FFT(image),150,150)
  ff=ABS(f)
  sum= ff(*,*) + sum
endfor
;------------- fft inverse   -----------------------------
```

```
  fsum    = shift( FFT(sum) ,150,150)
  afsum = ABS    (fsum)


;------------- contour --------------------------------
CNTRD, afsum ,     142 , 147     , xcen, ycen    , 1.5
print,xcen,ycen


;------------- write fit ----------------------------
figPath01 = 'D:\astro\data\20090317\hip64241\'
writefits,figPath01 + 'hip64241_img.fits'      ,    image    ; trans image
writefits,figPath01 + 'hip64241_sum.fits'      ,    sum        ; sum of all pic fft
writefits,figPath01 + 'hip64241_result.fits' ,    afsum    ; finial


print,'-------------ok---------------'
close,1


end
```

Appendix G   IDL Source code of tracking combine

```
pro track

file = 'D:\astro\data\20090629\track\we2.bmp'
z = READ_BMP(file,R,G,B,ihdr,/RGB)

nox=1024
noy=200

image=fltarr(nox,noy)
image=z

in=0
  for i=0,nox-1 do begin
    for j=0,noy-1 do begin
       if image(i,j) gt 250 then in=in+1
    endfor
  endfor

x=fltarr(in)
y=fltarr(in)

im=0
  for i=0,nox-1 do begin
    for j=0,noy-1 do begin
       if image(i,j) gt 250 then begin
         x(im)=i
         y(im)=j
         im=im+1
       endif
    endfor
  endfor

Xx=TRANSPOSE(x)
result = REGRESS(Xx , y , SIGMA=sigma, CONST=const,$
MEASURE_ERRORS=measure_errors)
```

```
xc=fltarr(2)
yc=fltarr(2)

xc(0)=0
yc(0)=result*xc(0) + const

xc(1)=nox-1
yc(1)=result*xc(1) + const

print,result
print,const
print,sigma

plot,x,y,xrange=[0,nox],yrange=[0,noy],psym=3,/isotropic,xstyle=1,ystyle=1,$
title='tracking', xtitle='pixel', ytitle='pixel',charsize=2
oplot,xc,yc,linestyle=0
legend,['Y=0.0367704X + 73.8935'],charsize=2,/left

print,'-------------ok---------------'

end
```

Appendix H IDL Source code of plot orbit

```
pro orbit_hip64241

close,1

!p.multi=[0,1,1,0,0]
aaa="
openr,1,'D:\astro\O_C\hip64241_4th.txt'
readf,1,aaa
nx=175
t_obs    =dblarr(1,nx)
obsrho   =dblarr(1,nx)
obstheta=dblarr(1,nx)

i=0
while not eof(1) do begin
   readf,1,format='(f9.4,2x,f5.2,2x,f7.5)',obsi,obsthetai,obsrhoi
   t_obs(i)=obsi
   obstheta(i)=obsthetai*!DTOR
   obsrho(i)=obsrhoi
   i=i+1
endwhile

x_obs=obsrho*cos(obstheta)
y_obs=obsrho*sin(obstheta)

i   =90.098d*!DTOR
o_1=192.235d*!DTOR
o_2=280.121d*!DTOR
p   =26.052d
T   =1989.2052d
ecc=0.5083d
a   =0.67633d
KA=a*(    cos(o_2)*cos(o_1) -sin(o_2)*sin(o_1)*cos(i)   )
KB=a*(    cos(o_2)*sin(o_1) +sin(o_2)*cos(o_1)*cos(i)   )
KF=a*(   -sin(o_2)*cos(o_1) -cos(o_2)*sin(o_1)*cos(i)   )
KG=a*(   -sin(o_2)*sin(o_1) +cos(o_2)*cos(o_1)*cos(i)   )
```

```
n1EE=2d*!dpi
stepEE=2d*!dpi/1000d
nEE=(n1EE/stepEE)+1

x_obi=DBLARR(1,nEE)
y_obi=DBLARR(1,nEE)



;--------------plot orbit of binary-----------
for EE=0,nEE-1 do begin
  X0=cos(EE*stepEE)-ecc
  Y0=((1-ecc^2)^0.5)*sin(EE*stepEE)
  x_obi(0,EE)=(KA*X0+KF*Y0)
  y_obi(0,EE)=(KB*X0+KG*Y0)
endfor


E=dblarr(1,nx)
for j=0,nx-1 do begin
  M=2.d*!dpi*(t_obs(j)-T)/P
  if M le   0        and M gt -2*!dpi   then   M=M +2*!dpi
  if M le -2*!dpi and M gt -4*!dpi   then   M=M +4*!dpi
  if M le -4*!dpi and M gt -6*!dpi   then   M=M +6*!dpi
  if M le -6*!dpi and M gt -8*!dpi   then   M=M +8*!dpi
  if M ge   2*!dpi and M lt   4*!dpi   then   M=M -2*!dpi
  if M ge   4*!dpi and M lt   6*!dpi   then   M=M -4*!dpi
  if M ge   6*!dpi and M lt   8*!dpi   then   M=M -6*!dpi

  Ec=!dpi
    for i=0,16 do begin
       if Ec-ecc*sin(Ec) gt M then begin
          Ec=Ec-(0.5d)^(i+1)*!dpi
       endif else begin
          Ec=Ec+(0.5d)^(i+1)*!dpi
       endelse
    endfor
  E(j)=Ec
endfor
```

```
X_c=cos(E)-ecc
 Y_c=((1-ecc^2)^0.5)*sin(E)
 xc=KA*X_c+KF*Y_c
 yc=KB*X_c+KG*Y_c

n = 17.0 ; the circle will be "created" with 17 data points (vertices)
theta = findgen(n)/(n-1.0)*360.0*!DtoR ;
x = 1.0*sin(theta)
y = 1.0*cos(theta)
usersym, x, y ,/fill

set_plot,'ps'
device,filename='D:\astro\O_C\hip64241.ps';,/color
plot,y_obi,x_obi,title='HIP 64241      P=26.052 years',xtitle='arcsec',ytitle='arcsec',$
/isotropic ,xrange=[-0.4,0.7],yrange=[-0.8,0.9],xstyle=1,ystyle=1
oplot,yc-yc,xc-xc,PSYM=1,symsize=2
oplot,y_obs,x_obs, PSYM=8,symsize=0.2
oplot,yc,xc,PSYM=3
usersym, x, y ;,/fill
plots,y_obs(174),x_obs(174), PSYM=8,symsize=0.5

for i=0, nx-1 do begin
  plots,[y_obs(i),yc(i)],[x_obs(i),xc(i)],linestyle=0;, /continue
endfor

device,/close
close,1
print,'------------- ok -------------'

end
```